THE UNIVERSITY OF IOWA

2003 Final Annual Report

Project No. CU1231

Fe(0)-Based-Bioremediation of RDX-Contaminated Groundwater

Submitted to:

Dr. Andrea Leeson

SERDP/ESTCP Cleanup Project Manager

901 N. Stuart Street, Suite 303

Arlington, VA 22203

703-696-2118 (V)

703-696-2114 (F)

andrea.leeson@osd.mil

by

Joshua D. Shrout, Brett Sutton, Leslie Sherburne, Phil Larese-Casanova, Michelle M. Scherer, Gene F. Parkin, Richard L. Valentine, Craig L. Just, and Pedro J.J. Alvarez*

Department of Civil and Environmental Engineering,

The University of Iowa, Iowa City, IA 52242-1527

Fax: (319) 335-5660

E-mail: pedro-alvarez@uiowa.edu

January 15, 2004

Report Documentation Page

Form Approved
OMB No. 0704-0188

1. REPORT DATE	2. REPORT TYPE	3. DATES COVERED
15 JAN 2004		**00-00-2004 to 00-00-2004**

4. TITLE AND SUBTITLE	5a. CONTRACT NUMBER
Fe(0)-Based-Bioremediation of RDX-Contaminated Groundwater	5b. GRANT NUMBER
	5c. PROGRAM ELEMENT NUMBER
6. AUTHOR(S)	5d. PROJECT NUMBER
	5e. TASK NUMBER
	5f. WORK UNIT NUMBER
7. PERFORMING ORGANIZATION NAME(S) AND ADDRESS(ES) **University of Iowa,Department of Civil and Environmental Engineering,Iowa City,IA,52242-1527**	8. PERFORMING ORGANIZATION REPORT NUMBER
9. SPONSORING/MONITORING AGENCY NAME(S) AND ADDRESS(ES)	10. SPONSOR/MONITOR'S ACRONYM(S)
	11. SPONSOR/MONITOR'S REPORT NUMBER(S)

12. DISTRIBUTION/AVAILABILITY STATEMENT
Approved for public release; distribution unlimited

13. SUPPLEMENTARY NOTES

14. ABSTRACT

15. SUBJECT TERMS

16. SECURITY CLASSIFICATION OF:			17. LIMITATION OF ABSTRACT	18. NUMBER OF PAGES	19a. NAME OF RESPONSIBLE PERSON
a REPORT	b ABSTRACT	c THIS PAGE			
unclassified	**unclassified**	**unclassified**	**Same as Report (SAR)**	**82**	

SUMMARY

RDX (hexahydro-1,3,5-trinitro-1,3,5-triazine) is an explosive compound that is gaining notoriety as a recalcitrant and toxic groundwater contaminant at many military installations. Batch and flow-through column studies suggest that permeable reactive iron barriers (PRBs) should effectively intercept and degrade RDX plumes, and that treatment efficiency could be enhanced by some biogeochemical interactions. This project addressesed the potential to enhance RDX degradation by bioaugmentation of an Fe(0) permeable reactive barrier, with focus on investigating RDX mechanisms and the sustainability and robustness of an integrated microbial-Fe(0) treatment system.

Activities completed this year included chemical characterization including assessing the subsequent "degradability" of unknown soluble metabolites formed during RDX transformation. Such byproducts were mineralized faster and to a greater extent to carbon dioxide than the parent RDX compound. A significant fraction of carbon from RDX formed under abiotic conditions was confirmed to be formaldehyde. We also continued to run flow-through column studies to investigate the sustainability of these systems. The RDX degradation profile for columns containing "aged" iron was determined and these columns were characterized with respect to their microbial communities and iron oxides formed along the length of the simulated Fe(0) barrier. Lastly, our investigation with the homoacetogen *Acetobacterium paludosum* has indicated that RDX can serve as a nitrogen source for this bacterium.

This report details the importance, relevance, and scope of this work and the achievement of milestones for this research in 2003.

INTRODUCTION

RDX is a recalcitrant and toxic contaminant present in the subsurface at many military installations. Because of its persistence, low tendency to volatilize (dimensionless Henry's constant, H' = 2×10^{-11}), and high mobility in aquifers (log K_{ow} = 0.8), clean-up of RDX-contaminated sites is a challenging problem. Several *ex situ* physical-chemical and biological practices to remove RDX from contaminated sites exist, but these are not cost-effective to treat large volumes of contaminated groundwater. In addition, complete destruction of RDX is not always achieved. The recalcitrance of RDX motivated this project to develop a new and efficient method to remediate RDX-contaminated aquifers. This method is based on combining a novel chemical process (reductive treatment with permeable Fe(0) barriers) with a promising bioremediation approach (*in situ* reactive zones). This integrated Fe(0)-microbial system should improve the capability and reduce the cost of RDX remediation.

SUMMARY OF WORK

Analysis of RDX Degradation Products

Batch experiments were conducted as described previously under both biotic and abiotic conditions to characterize the degradation of [^{14}C]-RDX. Throughout this project, several RDX degradation products have been identified, including mineralization products (CO_2 and N_2O) and transient nitroso intermediates (MNX, DNX, and TNX). A soluble RDX-degradation intermediate that we previously detected using both UV and radio-chromatographic detectors was also tentatively identified as methylenedinitramine (MEDINA) using LC/MS/MS (Figure 1). However, some soluble byproducts were not identified.

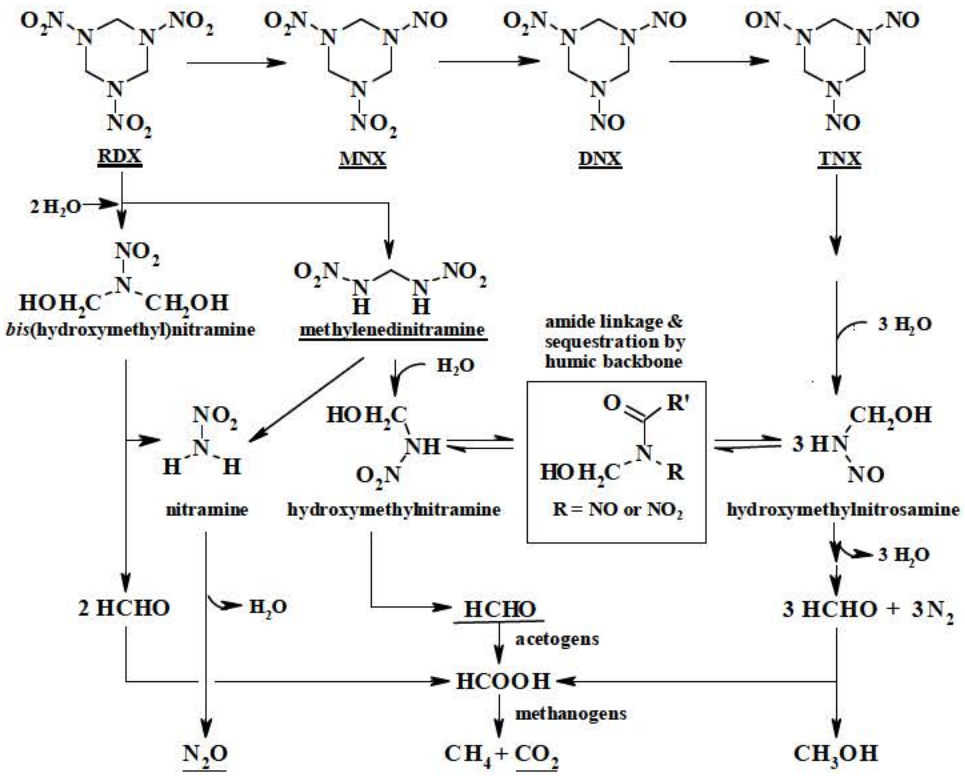

Fig. 1. Proposed RDX degradation pathway, based on work by Hawari et al.(2001). Species detected in this research are underlined (Source: Oh et al., 2001).

Experiments described below have yielded at least one additional metabolite that is not methylenedinitramine. RDX metabolite identification has been attempted using an Agilent 1100 series liquid chromatograph/mass spectrometer (LC/MS). Initial screenings have utilized full scan data acquisition in either positive or negative ion mode. A C18 column and 50/50 acetonitrile/water with 0.1% acetic acid at 1 mL/min was used for positive ion analysis. Acetic acid was replaced with ammonium acetate for negative ion analysis.

To date, with the exception of the identification of formaldehyde (which has been found to be a major byproduct in abiotic systems), identification efforts have been inconclusive mainly due to lack of MS sensitivity in full scan mode. The identification of unknown metabolites can

be a very difficult task, particularly if the compound(s) of interest are uncommon and not commercially available for verification and quantification as is the case here. Nevertheless, additional characterization was conducted by performing fundamental chemical investigation to determine the volatility and octanol-water partitioning of the RDX metabolite(s), was described below

Materials and Methods

High performance liquid chromatography (HPLC) analysis of RDX and its nitroso derivatives MNX, DNX, and TNX was performed using a Hewlett Packard 1100 Series HPLC equipped with a 250 x 4.6 mm Supelcosil^{TM} LC-18 column. The mobile phase consisted of deionized water and methanol (4:6, v/v) at a flow rate of 1.0 mL/min. UV detection was at 240 nm. [^{14}C]-RDX and its [^{14}C]-metabolites were analyzed by HPLC using a radioactivity detector (Radiomatic, Series A-500, Packard Instrument Co., Downers Grove, IL). RDX mineralization was determined from trapped [^{14}C]-CO_2 in the 0.5N NaOH tubes that were in the bottles.

Batch experiments were also conducted to investigate the degradability of ^{14}C-RDX degradation products eluting from the Bioaugmented column described below in *Column Studies,* and a separate ^{14}C-RDX metabolite from incubations with *Acetobacterium paludosum*. Mineralization assays were conducted under both aerobic and anaerobic conditions. Inoculums for some treatments consisted of soil collected from the University of Iowa Campus, Iowa City, IA. The soil was air dried for 24 hours and passed through a 1-mm sieve before use. The soil served as the source of indigenous microorganisms for the aerobic treatments. Additional microcosms were inoculated with activated and anaerobic sludge from the Iowa City South Waste Water Treatment Plant.

The synthetic groundwater medium for all microcosms contained (in mg/L): K_2SO_4 (40.0), NH_4Cl (16.0), $CaCl_2$ (6.66), $MgCl_2 \cdot 6H_20$ (12.2), K_2HPO_4 (3.48), H_3BO_3 (3.71×10^{-4}), $Ni(NO_3)_2 \cdot 6H_2O$ (1.74×10^{-3}), $CuSO_4 \cdot 5H_20$ (1.50×10^{-3}), $ZnSO_4 \cdot 7H_20$ (1.73×10^{-3}), $CoSO_4 \cdot 7H_20$ (1.69×10^{-3}), $(NH_4)_6Mo_7O_{24}$ (1.06×10^{-3}). The medium was buffered with $NaHCO_3$ (200) and the pH was adjusted to 7.0 units with HCl. Batch reactors used to investigate the mineralization of ^{14}C-labeled RDX degradation products contained the following: 2.5 mL of synthetic groundwater medium, 5.0 mL of diluted activated sludge (10% v:v, sludge:water), 5.0 mL of anaerobic sludge, and 12.5 mL of the unknown metabolite (0.007 μCi). RDX treatments contained the following: 13 mL of synthetic groundwater medium, 5.0 mL of diluted activated sludge (10% v:v, sludge:water), 5.0 mL of anaerobic sludge, 2.0 mg/L of ^{12}C RDX, and 0.007 μCi of ^{14}C RDX. All reactors contained 2.0 ml of 0.5 N NaOH in disposable glass tubes as a trap to collect CO_2 for monitoring the mineralization of RDX or the unknown metabolite. All of the 225-mL serum bottles were sealed with gray septa and aluminum crimps.

Metabolite products identified two separate RDX-degrading treatments described during previous quarters of this project were tested. The first unknown RDX-degradation metabolite composite was obtained from the Bioaugmented Column (as described in *Column Studies* below) effluent. Six treatment sets were monitored in duplicate: (1) unknown metabolite (UM-BC) and activated sludge, (2) UM-BC and anaerobic sludge, (3) UM-BC alone, (4) RDX and activated sludge, (5) RDX and anaerobic sludge, and (6) RDX alone.

Table 1: Description of Microcosms

Treatment	Description
1	UM-BC + activated sludge
2	UM-BC + anaerobic sludge
3	UM-BC (control)
4	RDX + activated sludge
5	RDX+ anaerobic sludge
6	RDX (control)

The second metabolite composite investigated was obtained during incubation of RDX with *Acetobacterium paludosum*. Six treatment sets were monitored in duplicate: (1) unknown metabolite (UM-AP) and soil, (2) UM-AP and anaerobic sludge, (3) UM-AP alone, (4) RDX and soil, (5) RDX and anaerobic sludge, and (6) RDX alone.

Table 2: Description of Microcosms

Treatment	Description
1	UM-AP + soil (aerobic)
2	UM-AP + sludge (anaerobic)
3	UM-AP (control)
4	RDX + soil (aerobic)
5	RDX+ sludge (anaerobic)
6	RDX (control)

All reactors were stored undisturbed at room temperature. Anaerobic treatments were purged for 15 minutes with N_2 to minimize dissolved gaseous oxygen. Addition of sludge, RDX, unknown metabolite, and NaOH traps was performed anaerobically. Anaerobic treatments were incubated quiescently in a Coy anaerobic chamber (28°C). Preparation of the sterile controls was performed aseptically in a laminar flow hood. Incubation was identical to that of the aerobic treatments. RDX mineralization was determined from trapped $^{14}CO_2$ by mixing 0.5 mL of sample with 9.5 mL of LSC cocktail (Fisher Scientific) and counting on a liquid scintillation counter (Beckman LS 6000IC).

High performance liquid chromatography (HPLC) analysis of RDX and its nitroso derivatives MNX, DNX, and TNX was performed using a Hewlett Packard 1100 Series HPLC equipped with a 250 x 4.6 mm Supelcosil^{TM} LC-18 column. The mobile phase consisted of deionized water and methanol (4:6, v/v) at a flow rate of 1.0 mL/min. UV detection was at 240 nm. [^{14}C]-RDX and its [^{14}C]-metabolites were analyzed by HPLC using a radioactivity detector

(Radiomatic, Series A-500, Packard Instrument Co., Downers Grove, IL). RDX mineralization was determined from trapped [^{14}C]-CO_2 in the 0.5N NaOH tubes that were in the bottles.

Results and Discussion

Two unidentified metabolites have been observed from the performed experiments (Table 3). A rigorous analysis of samples and known compounds has showed that these metabolites are not MEDINA. It is noteworthy that the metabolite observed at 3.1 minutes by HPLC analysis appears in both abiotic and biotic RDX-degrading treatments. The metabolite observed at 2.2 minutes by HPLC analysis is obtained only in some biotic systems.

Table 3. Characterization of RDX degradation products by studied abiotic and biotic systems.

Abiotic	**MNX**	**t***	**DNX**	**t***	**TNX**	**t***	**CO_2**	**t***	**Peak @3.1 min**	**t***	**Peak at 2.2 min**	**t***	**N_2O**	**t***	**NH_4**	**t***	**MEDINA**	**t***
Fe(II)/magnetite	17	500	35	750	33	2800	10	5300	90	2900	ND		ND		17	3800	ND	
Bioreduced Iron solids	41	200	19	250	9	600	5	2200	57	2200	ND		ND		5	1900	ND	
Sulfate Green Rust	15	0.5	21	0.5	6	0.5	NM	--	NM***	--	NM***	--	81	6	NM	--	NM	--
Biotic																		
***S. algae* BRY**	5	100	35	100	ND	100	<5	100	60	100	ND		NM		NM		ND	
A. paludosum	ND		ND		ND		<1	480	97	360	ND		NM		NM		NM	
***G. metallireducens* GS-15:**																		
MOPS-Fed	ND		ND		ND		42	3400	78	750	27	800	ND		NM		NM	
MOPS-Unfed	ND		ND		ND		11	3400	50	3500	10	3500	ND		NM		NM	
FC medium-fed	ND		ND		ND		12	3400	90	2000	ND		ND		NM		NM	
FC medium-unfed	ND		ND		ND		27	3400	90	2000	ND		ND		NM		NM	

Summary of products recovered in each experiment. Data are reported as percent (%) of initial RDX added. *t=time of measurement (hours).
Attempts to measure MEDINA used published methods (Hawari, et al. (2000); Oh et al. (2002). ND= Not detected. NM= Not measured.
*** these peaks could not be detected if present because the background peak for the buffer would have masked any other peaks near these elution times.

In an effort to learn more about the toxicity of the unknown metabolite(s), products formed by *A. paludosum* and *A. fimetarium* were investigated for their relative toxicity to RDX. This investigation was performed using a Microbics Microtox 500 Analyzer. The toxicity of samples containing the "3.1 minute" metabolite (see Table 3) were compared to a mix of metabolite and RDX to a positive and negative control. The samples used were taken from the previous mineralization experiment in which *A. paludosum* and *A. fimetarium* were exposed to approximately 2.7 mg/L RDX. Whereas there were initially six reactors in which bacteria were added (three with *A. paludosum*, and three with *A. fimentarium*), only four (two of each experimental condition) were still viable at the time of sampling. Thus the toxicities of the liquid samples from these four reactors were compared to the toxicities of two control samples. The positive (i.e., toxic response) control consisted of anaerobic medium amended with RDX and the negative control contained the same anaerobic medium without RDX. The initial pH of all samples was adjusted near circumneutral using 5N HCl. Table 4 describes the RDX-metabolized samples tested.

Table 4. Microtox Sample Information

Sample	Approximate pH	RDX (mg/L)	Metabolite % Peaks HPLC-RAD (3.1 minute peak)
Medium	6.8	0	0
Medium with RDX	6.8	3.64	0
A. Paludosum	7.1	0 (initial RDX 2.7 mg/L)	98
A. Paludosum (dupl.)	6.8	0 (initial RDX 2.7 mg/L)	97
A. Fimentarium 1	6.8	1.4 (initial RDX 2.9 mg/L)	50
A. Fimentarium (dupl.)	6.8	1.6 (initial RDX 2.8 mg/L)	45

The Microtox test determines the toxicity of a sample to a well-characterized, bioluminescent, marine bacterium, *Photobacterium phosphoreum*. Prior to the assay, bacteria were grown under optimal conditions as per the Microtox protocol, harvested, then lyophilized.

Before starting a test, the bacteria are rehydrated using Microtox Reconstitution Solution. Once hydrated, the bacteria are viable for approximately 5-8 hours.

The assay involves incubating the rehydrated bacteria with the test sample. The light output of the bacteria exposed to the sample is compared to the light output of the negative and positive controls. The principle of the test is that the toxicity of a sample is indirectly proportional to the light production, that is, the more toxic the sample, the less light will be produced.

A dose-response curve from the data collected can then be used to find the EC50 under a specific exposure time and test temperature (which is always 15 ^{o}C for this model analyzer). The EC50 is the effective concentration of a sample at which the light output is reduced by 50%. Thus a higher EC50 value means a less toxic compound, and vice versa. The EC50 is often recorded after the bacteria are exposed to the sample for 5 minutes and for 15 minutes.

Microtox data for these samples revealed no significant statistical difference between RDX and formed compounds, however there appeared to be a trend towards lower toxicity in samples containing metabolized RDX. Further investigation will be required to verify this potential trend. The results suggest that the formed RDX metabolite is not more toxic than parent RDX. Figure 2 shows the estimated EC50 values for the performed assays. The error bars shown indicate a 95% confidence range.

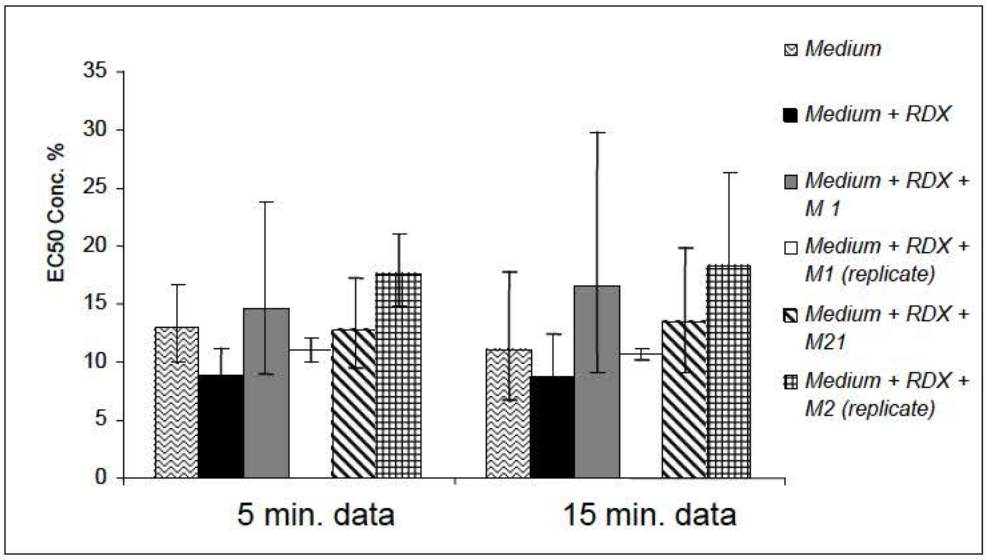

Fig. 2. EC50 Concentrations of RDX and RDX-metabolized samples by Acetobacterium species by Microtox assay. M1 = metabolite generated from *A. paludosum*. M2 = metabolite generated from *A. fimentarium*.

Batch experiments were conducted to characterize the transformation of RDX by *Acetobacterium paludosum*. When RDX is transformed by these bacteria, two or more unknown soluble metabolites are formed. Additional significant findings of these experiments are detailed later in this report.

The unknown metabolites were investigated to verify they are unique and not a previously determined RDX-degradation intermediate. Samples of the unknown chemical were compared to several known compounds, including formaldehyde, formic acid, methanol, MNX, DNX, and TNX by HPLC or HPLC-RAD to determine if their retention times were close to those of the unidentified metabolite(s). The retention times of these compounds and those of the unidentified metabolite(s) are presented in Table 5 and suggest that the metabolite is not any of these compounds.

RDX metabolite identification has also been attempted using an Agilent 1100 series liquid chromatograph/mass spectrometer (LC/MS). Initial screenings have utilized full scan data

acquisition in either positive or negative ion mode. A C18 column and 50/50 acetonitrile/water with 0.1% acetic acid at 1 mL/min was used for positive ion analysis. Acetic acid was replaced with ammonium acetate for negative ion analysis.

Table 5: Comparison of retention times of metabolite(s) with possible RDX degradation products

Compound(s)	*Retention Time (min)*	*Analysis*
Metabolite(s)	2.7	HPLC-RAD
MNX	5.6	HPLC
DNX	5.4	HPLC
TNX	5.2	HPLC
Formaldehyde*	6.0	HPLC-RAD
Formic Acid	2.8	HPLC-RAD
Methanol	2.7	HPLC-RAD

* After derivatization (EPA method #8315A)

To date, identification efforts have been inconclusive mainly due to lack of sensitivity in full scan mode. If this project had been continued, future analyses would have utilized selected ion monitoring (SIM), one ion at a time, to improve sensitivity. The sensitivity improvement afforded using SIM results in a dramatic decrease in structural information. Metabolite identifications would have been confirmed by stable isotope analysis using ^{13}C- and ^{15}N-RDX.

Additional metabolite characterization was conducted by performing fundamental chemical investigations to determine the volatility, reactivity in the presence of oxygen, and octanol-water partitioning of the RDX metabolite(s). Based upon recoveries of ^{14}C compared to added concentrations, results obtained show that the metabolite(s) is not volatile, does not react with oxygen, and has an octanol-water coefficient of -1.87, which indicates that it is very water soluble (and not likely to fix to soil). It should be noted that the octanol-water coefficient is only relevant if there is only one metabolite compound. If there is more than one chemical constituent present in these samples, the determined K_{ow} is not accurate and it would reflect a weighted average. These characteristics are summarized in Table 6.

Table 6: Selected properties of the metabolite(s)

	Volatility	*Reactivity with O_2*	*Log K_{ow}*
Metabolite(s)	None observed	None observed	-1.87

Additional samples have been characterized from abiotic batch studies investigating the degradation of RDX with green rusts. (Other significant findings of these experiments are described in a following section.) Aqueous samples were analyzed for ^{14}C radioactivity using a radiochem detector following HPLC-UV analysis. ^{14}C-RDX and some of its transformation products separated within the C-18 chromatography column appeared as peaks in the radiochem chromatogram. After 20 minutes, most of the ^{14}C radioactivity appears in the peak with a retention time of 2.9 minutes (Fig. 3). A similar peak has been observed in microcosms containing RDX and pure cultures of homoacetogens as well as in reactor vials containing RDX and synthetic magnetite with dissolved Fe^{2+}. A smaller peak also occurs at 3.6 minutes, followed by a peak at 8.2 minutes that corresponds to ^{14}C-RDX. After derivatization for HCHO analysis (EPA method #8315A), most of the ^{14}C radioactivity shifted from 2.9 min to 6.0 min reflecting the HCHO-DNPH derivative (Fig. 3). The shift suggests that most of the ^{14}C radioactivity in the original 2.9 min peak is HCHO. The RDX peak, the 3.6 min peak, and residual 2.9 min peak are still apparent after derivatization (a higher composition of acetonitrile in the eluent for derivatization was responsible for reduced retention times). Potential RDX transformation products present within the 3.6 min peak are currently being evaluated using LC/MS techniques.

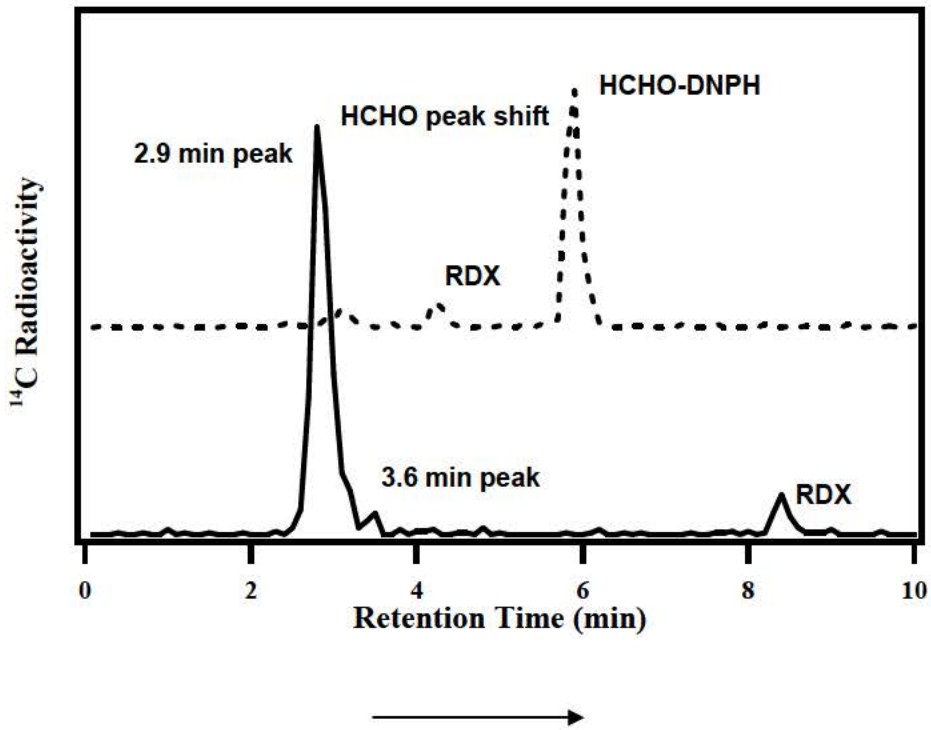

Fig. 3. Radiochem chromatograms for an aqueous sample taken at 20 minutes (solid line) and an aqueous sample at 20 minutes after DNPH derivatization for HCHO analysis (dashed line).

The metabolite UM-BC from Bioaugmented Column effluent was mineralized under both anaerobic and aerobic conditions after two weeks (Fig. 4). Recovery of $^{14}CO_2$ was greater from UM-BC treatments than for RDX under both anaerobic and aerobic conditions, implying that RDX degradation byproducts that break through an iron barrier have a greater potential for natural attenuation than the parent RDX compound. A minimal amount of RDX degradation was observed around 8 days and this was possibly due to spillage from the NaOH trap that caused alkaline hydrolysis of RDX. Less than 2% $^{14}CO_2$ was recovered in non-inoculated controls.

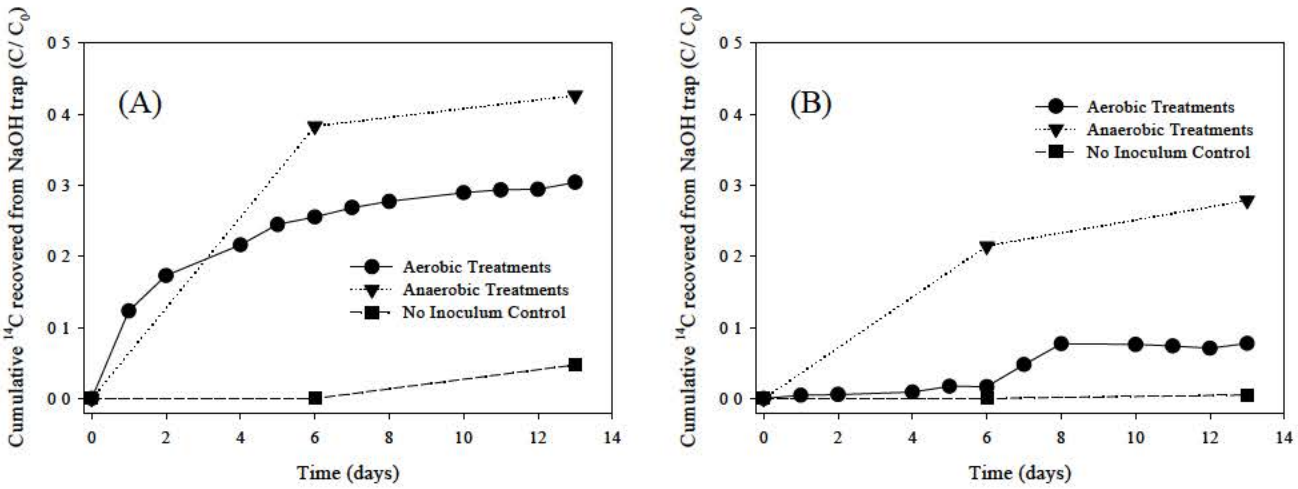

Fig. 4. Mineralization of (A) Unknown Metabolite (UM-BC) (0.007 μCi) from Column Effluent and (B) RDX incubated in separate batch microcosms. (2.0 mg/L, 0.007 μCi).

The ORP of Aerobic and Anaerobic treatments was measured over time to verify that aerobic or anaerobic environments prevailed during the UM-BC mineralization assays. Table 7 shows the ORP measurements, indicating that this was the case.

Table 7. ORP of UM-4.6 Degradability Treatments (mV)

time	Metabolite UM-4.6			RDX	
(days)	aerobic	anaerobic		aerobic	anaerobic
0	127.8	69.3		109.7	53.9
1	168.9	-		146.35	-
2	192.6	-		150.75	-
4	215.5	-		147.9	-
5	266.9	-		156.2	-
6	265.8	-234.4		164.35	-291.7
7	193.1	-		140.25	-
13	223.5	-280.4		194.45	-331.7

The metabolite(s) UM-AP produced by *Acetobacterium paludosum* was mineralized under both anaerobic and aerobic conditions after three weeks (Fig. 5). Mineralization was greater under anaerobic conditions. Recovery of $^{14}CO_2$ was greater from UM-2.3 treatments than for RDX under anaerobic and aerobic conditions, respectively. Less than 3% $^{14}CO_2$ was recovered in non-inoculated controls.

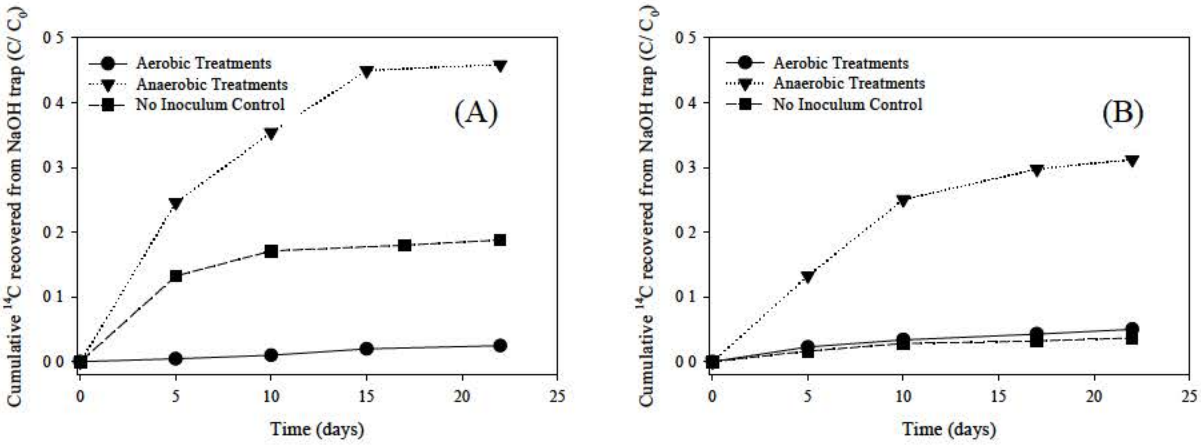

Fig. 5. Mineralization of (A) Unknown Metabolite (UM-AP) (0.63 μCi)from RDX Degradation by *Acetobacterium paludosum* and (B) RDX (1.0 mg/L, 0.6 μCi) incubated in separate batch microcosms.

Chemical analyses were conducted to determine if formaldehyde is a byproduct of RDX degradation by *S. alga* BrY or its biogenic iron mineral. The formaldehyde derivitization procedure (EPA method #8315A) was used for this purpose. As previously reported, the majority of the RDX-derived ^{14}C was associated with an unknown metabolite. This metabolite, however, was not formaldehyde.

In summary, although some unknown RDX degradation byproducts remain elusive, valuable information was obtained regarding their solubility and high mineralization potential, as well as their relatively low ecotoxcicity. Overall, this information together with previous mineralization data suggest that RDX degradation in and around bioaugmented Fe(0) PRBs is a safe process, and that the predominant transformation products are more biodegradable and less toxic than the parent compound.

Column Studies

Background

Flow-through columns were started in November 2000 to evaluate the efficacy of permeable reactive iron barriers to treat groundwater contamination by RDX. We also used these columns to evaluate the overall effect of microbial processes (e.g., growth and mineral dissolution/precipitation) on the permeability and efficiency of Fe(0) barriers.

Materials and Methods

Four columns (30-cm long, 2.5-cm ID) equipped with lateral sampling ports were packed with a 5-cm layer of soil (Iowa Army Ammunition Plant, Middletown, IA) followed by an 18-cm layer of Master Builder® Fe(0) filings (representing a reactive barrier) and a 7-cm sand layer (Fig. 6). One of the columns was poisoned with $HgCl_2$ (200 mg/L), sodium azide (200 mg/L), and a biocide (Kathon, 1 mL/L) to limit biological growth and investigate degradation by Fe(0) alone. The second (non-sterile) column was used to determine if soil bacteria colonize the Fe(0) layer, presumably to feed on cathodic H_2 produced by anaerobic Fe(0) corrosion. This column also serves as a baseline to evaluate the benefits of bioaugmentation. The third column was inoculated with municipal anaerobic sludge (10 mL of stock (6.6 g-VSS/L) added at each port) to enhance reductive treatment of RDX. The fourth column was prepared with inert glass beads instead of Fe(0) to control for the effect of indigenous microorganisms on RDX degradation. RDX (^{14}C-labeled) has been fed continuously at 17 mg/L (10 μCi/L) at 2.3 mL/hr (about 0.5 ft/day superficial velocity) with bicarbonate-buffered synthetic groundwater (von Gunten and Zobrist, 1993) using a peristaltic pump.

High performance liquid chromatography (HPLC) analysis of RDX was performed using a Hewlett Packard 1100 Series HPLC equipped with a 250 x 4.6 mm Supelcosil™ LC-18 column. The mobile phase consisted of deionized water and methanol (4:6, v/v) at a flow rate of 1.0 mL/min. UV detection was at 240 nm. [^{14}C]-RDX and its [^{14}C]-metabolites were analyzed by HPLC using a radioactivity detector (Radiomatic, Series A-500, Packard Instrument Co., Downers Grove, IL). Bromide was analyzed by ion chromatograph (IC) using a DIONEX AS-14 column where separation was achieved by an eluent of carbonate (370 mg/L) and bicarbonate (84 mg/L) at a flow rate of 1.5 mL/ min.

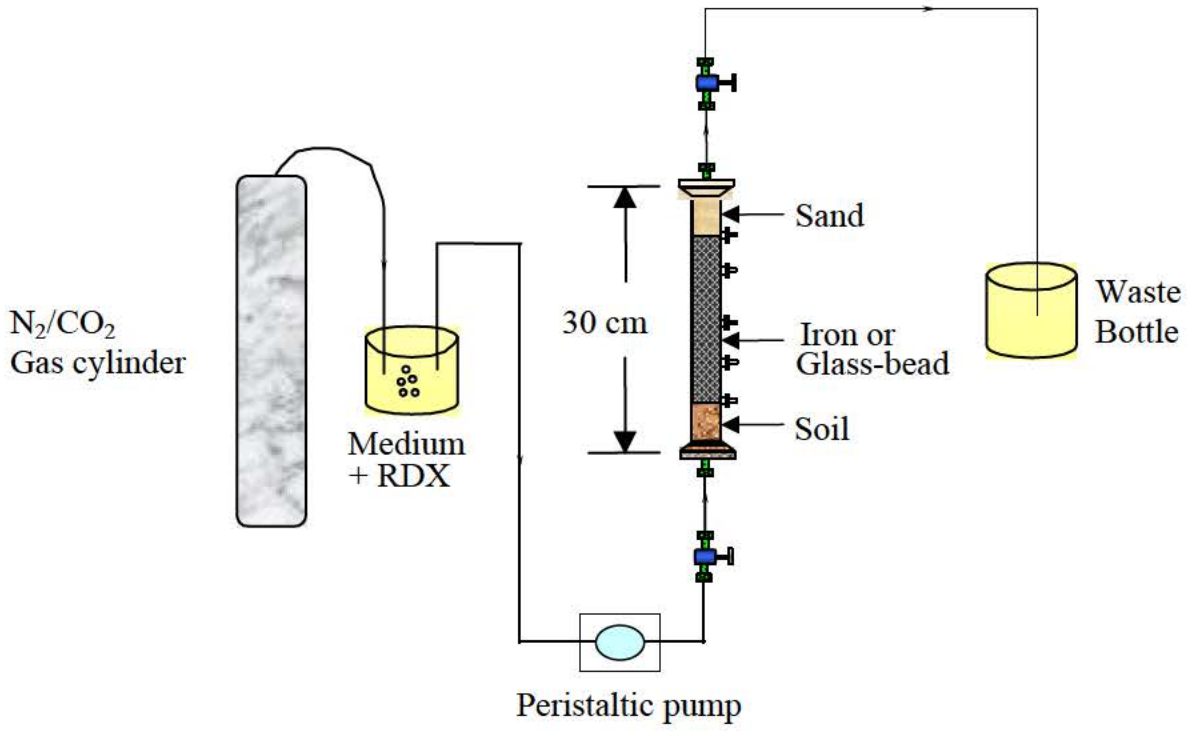

Fig. 6. Flow-through columns used to simulate permeable reactive iron barriers.

Results and Discussion

These four columns continue to be maintained and operated with an influent feed solution of approximately 15 mg/L RDX. Previous results have suggested the potential for complete

mineralization by the two columns with promoted biological activity. High removal efficiencies for both the indigenously colonized column and the bioaugmented column have been sustained for two years, and in fact have been improving presumably due to enhanced acclimation of the microbial consortium and proliferation of competent strains. This will continue to be monitored. The longevity of this performance suggests such treatment by bioaugmentation of Fe(0) is sustainable over time.

The dissolved ^{14}C activity remained unchanged in the control column packed with inert glass beads (Fig. 7). This suggests that RDX was not transformed in the absence of Fe(0) or anaerobic sludge, and that it was not strongly sorbed or naturally attenuated in the soil layer either. All columns containing Fe(0) removed RDX below detectable levels within a few centimeters of the entrance to the iron layer, although a significant residual radiolabel concentration was observed. The results suggest the potential for complete mineralization by the two columns with promoted biological activity. Both the Naturally Colonized (i.e., indigenous organisms) and Bioaugmented columns have shown complete degradation of RDX and a decrease in the aqueous RDX-metabolized products during the period investigated. Removal of soluble ^{14}C has remained stable for greater than 2 years in the biological columns. One likely remaining product, not measured for these columns, is bicarbonate (i.e., dissolved carbon dioxide gas), suggesting complete mineralization of added RDX.

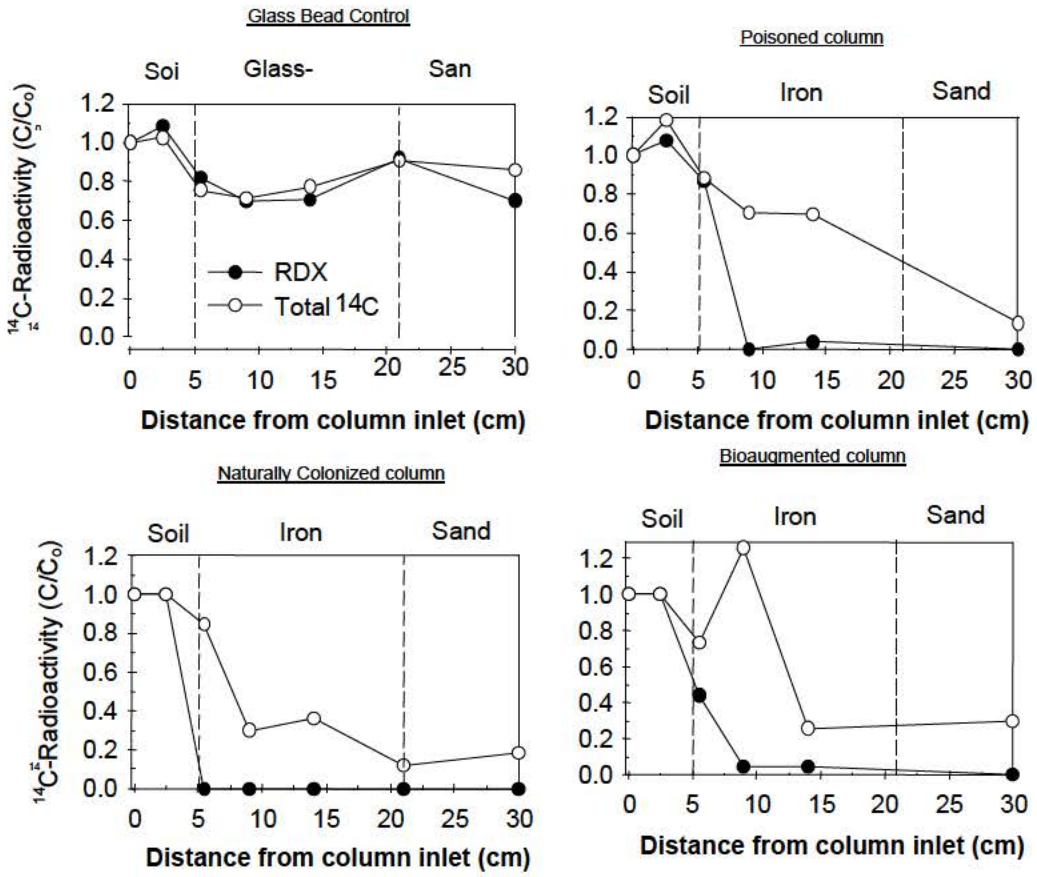

Fig. 7. RD X concentration and soluble ^{14}C activity after 32 months of operation (C_0 = 10 mg/L and 10 μCi/L). The hydraulic retention time through the columns was approximately 1.5 days.

The poisoned column showed a relatively high decrease in dissolved ^{14}C activity. This decrease may be due, in part, to microbial activity (e.g., mineralization and/or humification into soil), reflecting the difficulty to keep open systems completely sterile. The Naturally Colonized column showed a high decrease in dissolved ^{14}C activity at the effluent (80% removal efficiency). The bioaugmented column also exhibited a high removal of dissolved ^{14}C activity (~70%). The loss of soluble ^{14}C is possibly due to microbial-mediated mineralization in these columns as shown previously in batch studies containing both iron and bacteria. As high removal efficiencies have been sustained for two years this suggests the acclimation of the microbial consortium and proliferation of competent strains. The longevity of this performance suggests such treatment by bioaugmentation of Fe(0) is sustainable over time.

The hydraulic characteristics of the columns were determined from bromide tracer studies (NaBr). Such tracer studies will provide a baseline for future determination of changes in permeability in different columns. A bromide (Br^-) solution (50 mg Br^-/L) was continuously fed through packed columns using a peristaltic pump. Effluent samples were collected every hour with an auto sampler. Effluent bromide concentrations were monitored by ion chromatography until they reached influent levels. Bromide breakthrough curves were used to calculate the effective porosity (η_e), dispersion coefficient (D) and retardation factors (R_f) by fitting the breakthrough data to the 1-D advection-dispersion equation (Domenico and Schwartz, 1998):

$$C = \left(\frac{Co}{2}\right) erfc\left[\frac{\left(R_f x - \left(\frac{Q}{A?_e}\right)t\right)}{2\sqrt{DR_f t}}\right] + \exp\left[\left(\frac{Q}{A?_e}\right)\frac{x}{D}\right] erfc\left[\frac{\left(R_f x + \left(\frac{Q}{A?_e}\right)t\right)}{2\sqrt{DR_f t}}\right] \quad \text{(Eq.1)}$$

Where C is the effluent concentration, Co is the influent concentration, x is the column length, t is the elapsed time, Q is the flow rate, A is the cross sectional area, and erfc is the complementary error function.

The tracer curves clearly showed that the interconnected pore volume (and the associated effective porosity) has experience some fluctuation over the 32-month operation of these columns (Fig. 8). These changes do not necessarily reflect changes in total porosity since other processes such as gas production and bubble formation could have a significant impact on hydraulic properties. Shifts in the breakthrough curves towards the left indicate that the interconnected pore volume (which corresponds to $C/C_0 = 0.5$) has decreased, this is possibly due to oxide deposition, gas bubbles (e.g., H_2) and/or microbial growth. Conversely, a shift to the right corresponds to a porosity increase possibly due to iron dissolution or gas bubbles consumption. The effective porosity has decreased only a small amount in the bioaugmented

column and shows no change in the naturally colonized column after 32 months operation. No problems with clogging have ever been observed with the columns. In combination with the favorable RDX degradation observed over time in biologically active columns, these results suggest sustainability of this bioaugmented iron scheme.

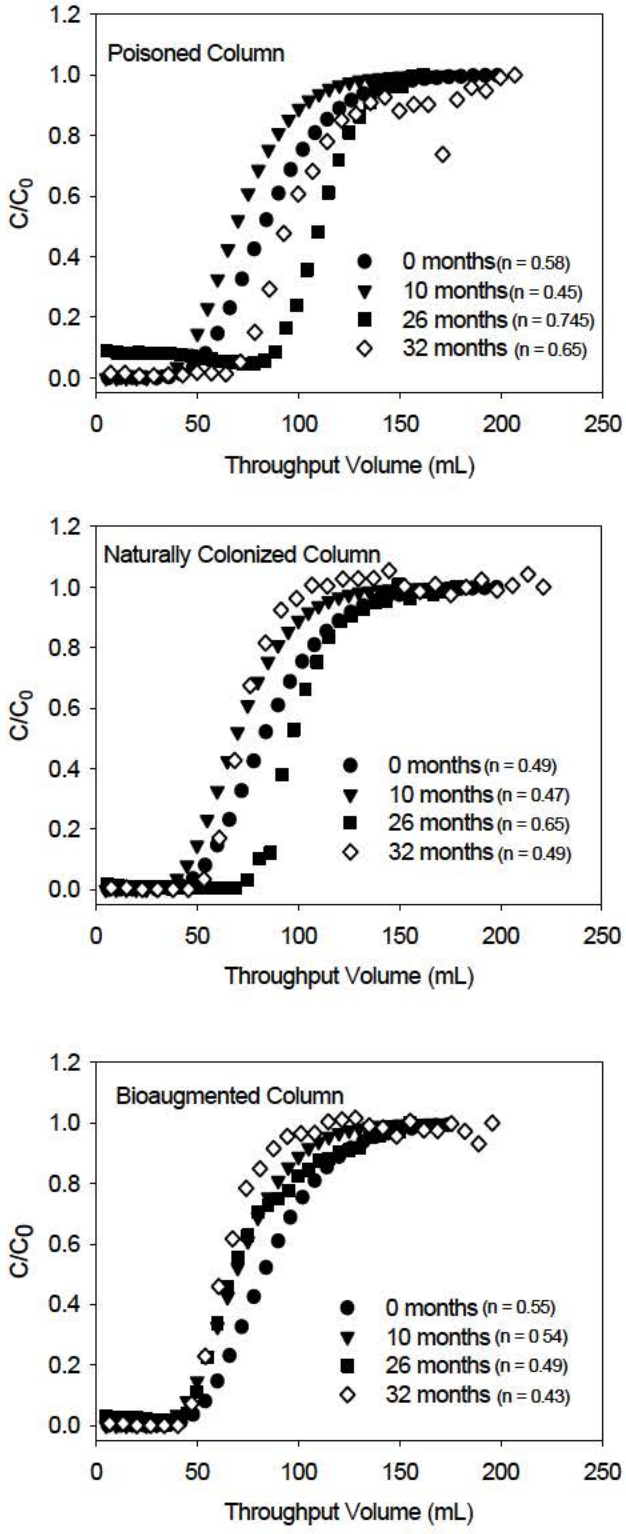

Fig. 8. Tracer studies for three flow-through columns simulating a permeable reactive iron barrier (C_0 = 50 mg/L Br^-).

Characterization of "Aged" Fe(0) Column Bioaugmented with Iron Reducers

Background

In order to determine if dissimilatory iron-reducing bacteria (DIRB) enhance barrier reactivity by reductive dissolution of Fe(III) oxides or by formation of reactive oxides, we inoculated two additional iron columns with DIRB. These columns were packed with "aged" iron obtained from columns that had been exposed to TCE, Cr(VI), sulfate, and nitrate mixtures for 1 year (Gandhi et al, 2002). This iron was used to mimic iron that has been aged in a reactive barrier over time, which could be amenable for reactivation by DIRB.

Materials and Methods

Regarding this additional column experiment, three columns (30-cm long, 2.5-cm ID) equipped with lateral sampling ports were packed with a 5-cm layer of soil followed by an 18-cm layer of the aged iron previously described, and a 7-cm sand layer as described in Fig. 5. Uncontaminated soil was obtained from the field in Iowa City, IA. One of the columns was used to determine if soil bacteria colonize the Fe(0) layer, presumably to feed on cathodic H_2 produced by anaerobic Fe corrosion. This column also serves as a baseline to evaluate the benefits of bioaugmentation. The second column was inoculated with the iron-reducing bacterium *Shewanella algae* BRY (10 ml of stock (52.6 mg protein/L) added at each port). The third column was inoculated with the iron-reducing bacterium *Geobacter metallireducens* GS-15 (10 ml of stock (36 mg protein/L) added at each port). While *S. algae* can grow autotrophically on hydrogen, *G. metallireducens* can only grow under heterotrophic conditions (Lovley, et al., 1993).

These strains were inoculated to determine if DIRB enhance barrier reactivity by

reductive dissolution of Fe(III) oxides or by formation of reactive oxides. RDX (^{14}C-labeled) has been fed continuously at 18 mg/L (10 μCi/L) at 2.3 mL/hr (about 0.5 ft/day superficial velocity) with bicarbonate-buffered synthetic groundwater (von Gunten and Zobrist, 1993) using peristaltic pump.

Results and Discussion

We have monitored RDX removal along the length of the columns by sampling the side ports and analyzing the samples by HPLC. RDX concentration profiles for 65 and 250 days showed extensive and sustainable RDX removal in all columns with aged iron filings. The column colonized by indigenous bacteria showed a decrease in dissolved ^{14}C activity along its length (Fig. 9). The column inoculated with *Shewanella algae* BRY exhibited a higher removal of dissolved ^{14}C activity than the one bioaugmented with *Geobacter metallireducens* GS-15. This suggests that *Shewanella algae* BRY might be able to enhance barrier reactivity faster than *Geobacter metallireducens* GS-15, although it is unclear if this is due to higher reductive dissolution of passivating oxides or to their transformation to more reactive forms (e.g., magnetite, green rust, and other forms of surface-bound Fe(II) (Gerlach, et al., 2000)). Whether BRY participates directly in RDX degradation (perhaps using it as a nitrogen source) will be addressed later in this report.

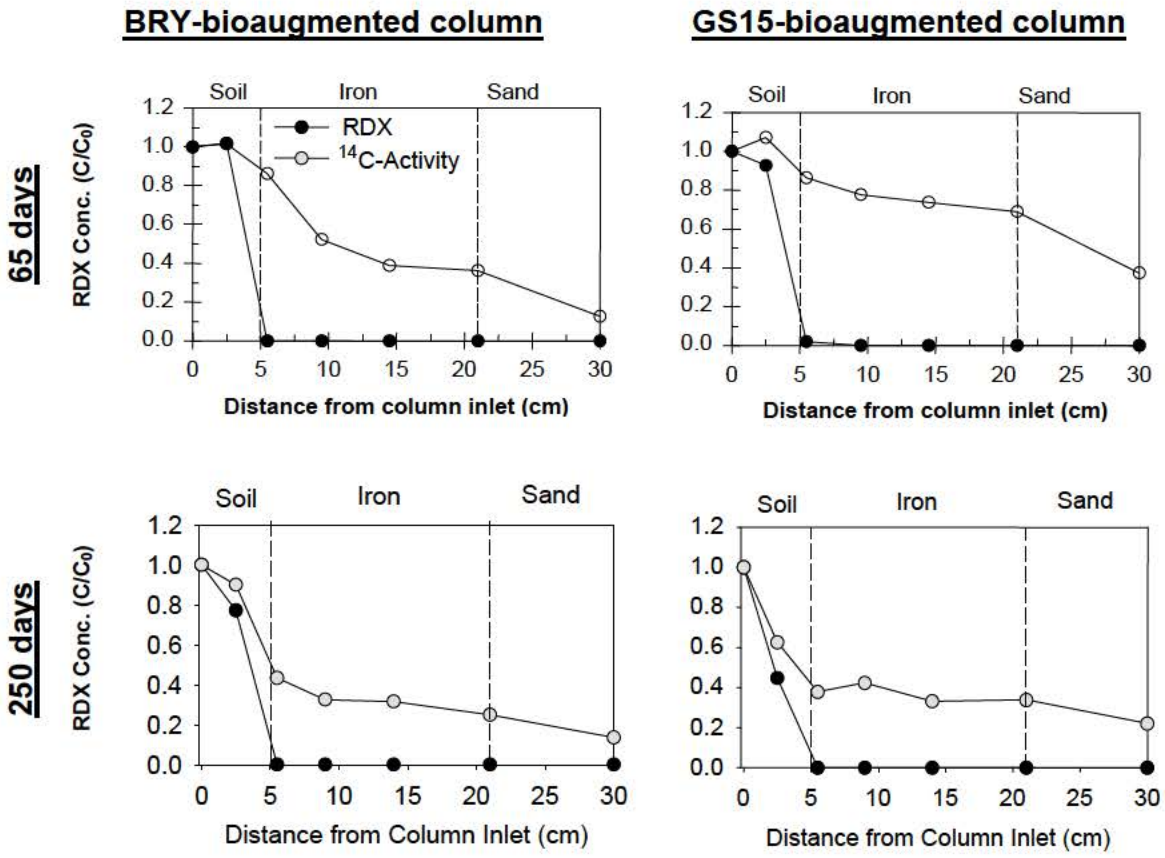

Fig. 9. Change of RDX concentration and soluble ^{14}C activity using rusted Fe after 65 and 250 days of operation. (C_0 = 18 mg/L and 10 μCi/L).

The columns were dismantled after 27 months operation. RDX was removed in all columns and the RDX concentration profiles after 370 days shows extensive and sustainable RDX removal (Fig. 10, 11, and 12). A comparison over time of these columns shows degradation of RDX closer to the column inlet on day 370 than on day 65 (reported in the previous quarterly report). RDX degradation was more complete in the bioaugmented columns and required less time to show higher removal of soluble ^{14}C, suggesting more mineralization of RDX. The ability to degrade and mineralize RDX improved in all columns over a one-year period, possibly due to microbial acclimation and growth. Enhanced performance associated with DIRB bioagumentation may also be due to reductive dissolution of passivating oxides and

their transformation to more reactive minerals (e.g., green rust, maghemite, siderite, and other forms of surface-bound Fe(II)).

Four unknown ^{14}C metabolites were identified in these samples. Unknown 1 likely contains multiple compounds as LC/MS results suggest a mass consistent with MDNA (m/z = 181) was present in Unknown 1, but not in sufficient quantity to represent all ^{14}C recovered. Unknown 2 was tentatively identified as formaldehyde, based on a derivatization procedure (EPA Method 8315A).

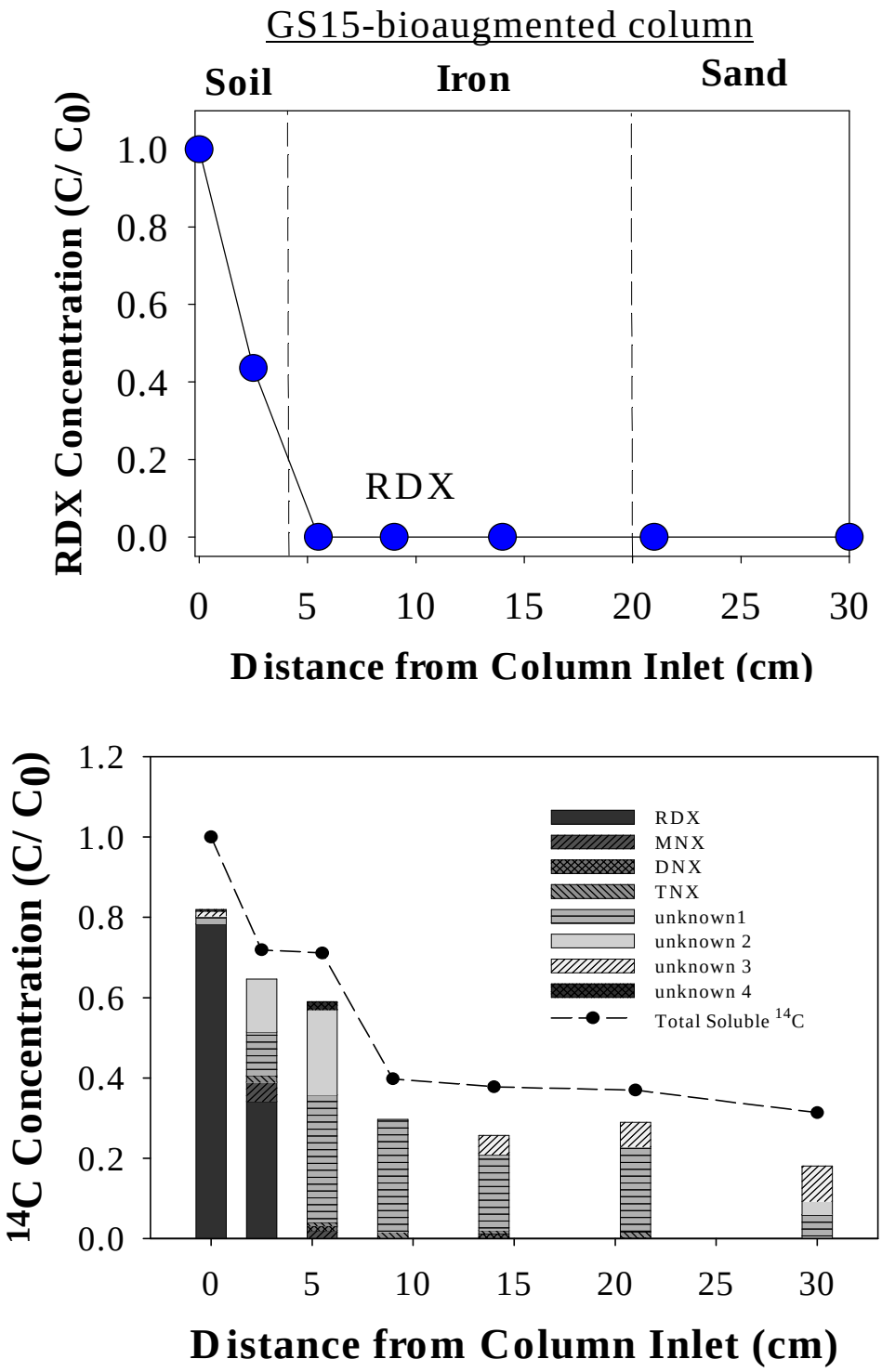

Fig. 10. RDX, formed metabolites, and total ^{14}C versus distance for flow-through Fe(0) barrier column bioaugmented with *G. metallireducens* GS-15 operated for 370 days. (C_0 = 16 mg/L and 10 µCi/L)

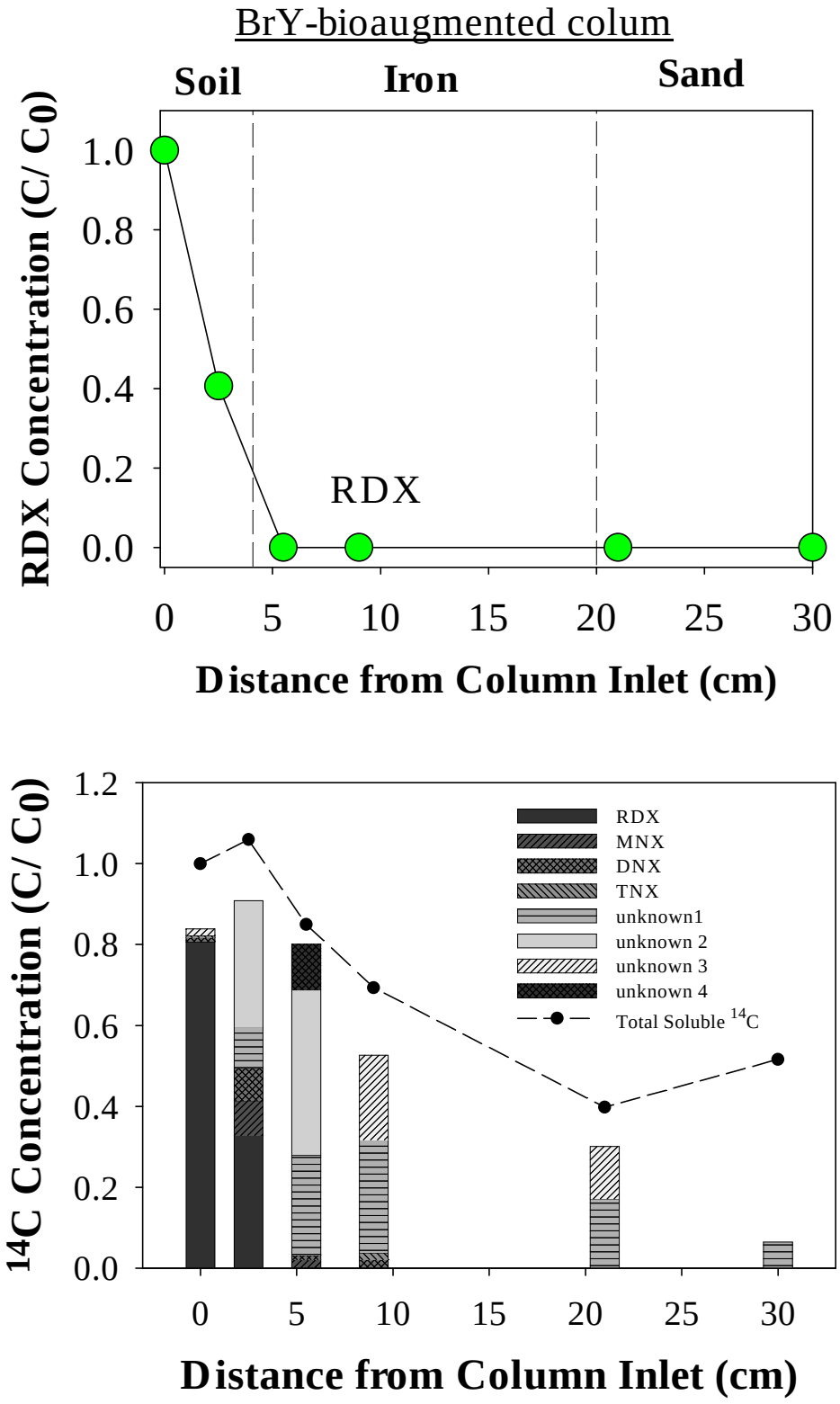

Fig. 11. RDX, formed metabolites, and total ^{14}C versus distance for flow-through Fe(0) barrier column bioaugmented with *S. algae* BrY operated for 370 days. (C_0 = 16 mg/L and 10 μCi/L)

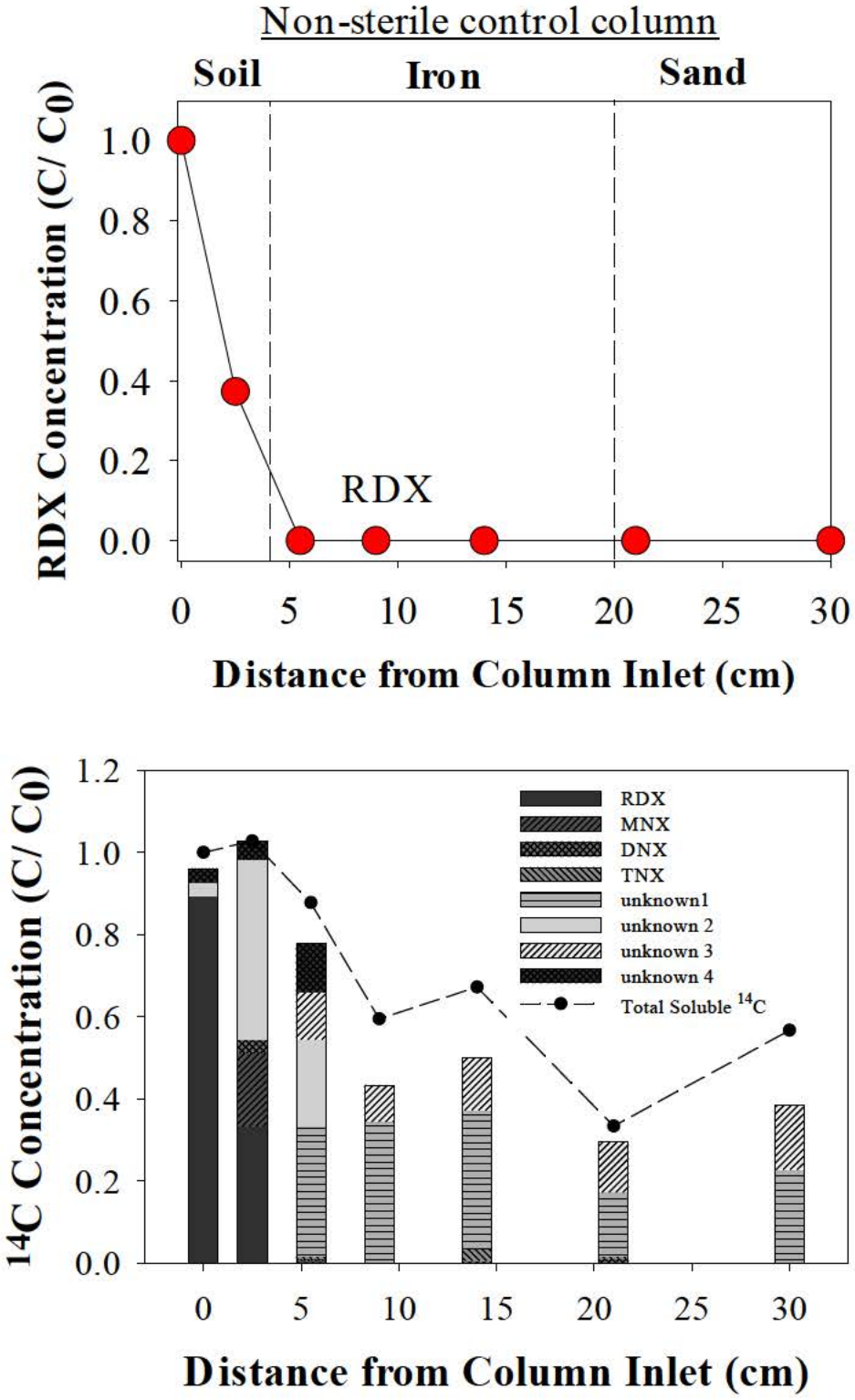

Fig. 12. RDX, formed metabolites, and total ^{14}C versus distance for flow-through Fe(0) barrier "control" column naturally colonized by indigenous bacteria operated for 370 days. (C_0 = 16 mg/L and 10 μCi/L)

It is currently unclear the roles that *Shewanella algae* BRY and *Geobacter metallireducens* GS-15 have played in these columns, if any, but it is possible that these bacteria contributed to some degradation of RDX, reductive dissolution of oxides that would passivate the iron, and transformation of iron species to more reactive forms (e.g., magnetite, green rust, and other forms of surface-bound Fe(II) (Gerlach, et al., 2000). Production of siderite and magnetite/maghemite were reported previously for pure cultures of *Geobacter metallireducens* GS-15 and *Shewanella algae* BRY (Annual Report, 2002).

16S rDNA was recovered from all columns at all sampling points. Separation of DNA using DGGE shows the recovery of multiple species along the length of all three columns (Fig 13). Two primer sets were utilized to off-set any bias of one particular primer set for specific bacterial genera, such that a more complete investigation of colonized species might be performed. The recovery of multiple bands from the high-pH Fe(0) areas and post-Fe(0) sand region of the columns was unexpected given the relatively high pH encountered along the length of these columns (Fig 14). This DNA recovery shows the presence of bacteria in these regions. Sequences could not be determined due to the complex nature of the samples and the difficulty to recover and purify DNA when high iron concentrations are present. Optimization of DGGE and DNA recovery techniques by Microbial Insights, Inc, was not successful either (other than to confirm that the columns had been colonized by microorganisms). Thus, the identity of the bacteria species present in these columns could not be determined, which precluded the assessment of the survival of added DIRB, primarily due to low DNA recovery..

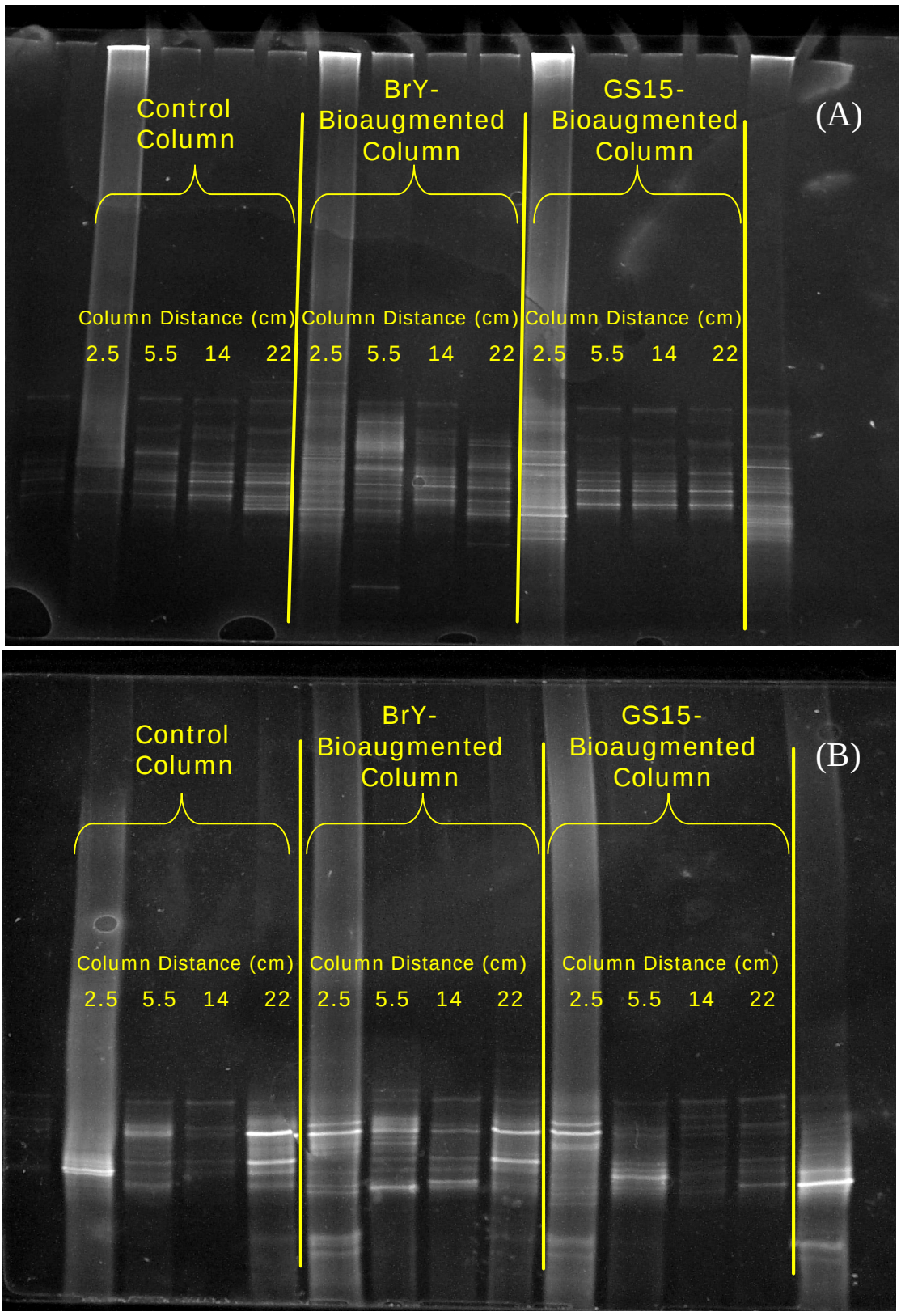

Fig. 13. DGGE of 16S rDNA amplified using primers (A) 341F and 907R and (B) 1055F and 1392R for Fe(0) barrier columns operated for 370 days.

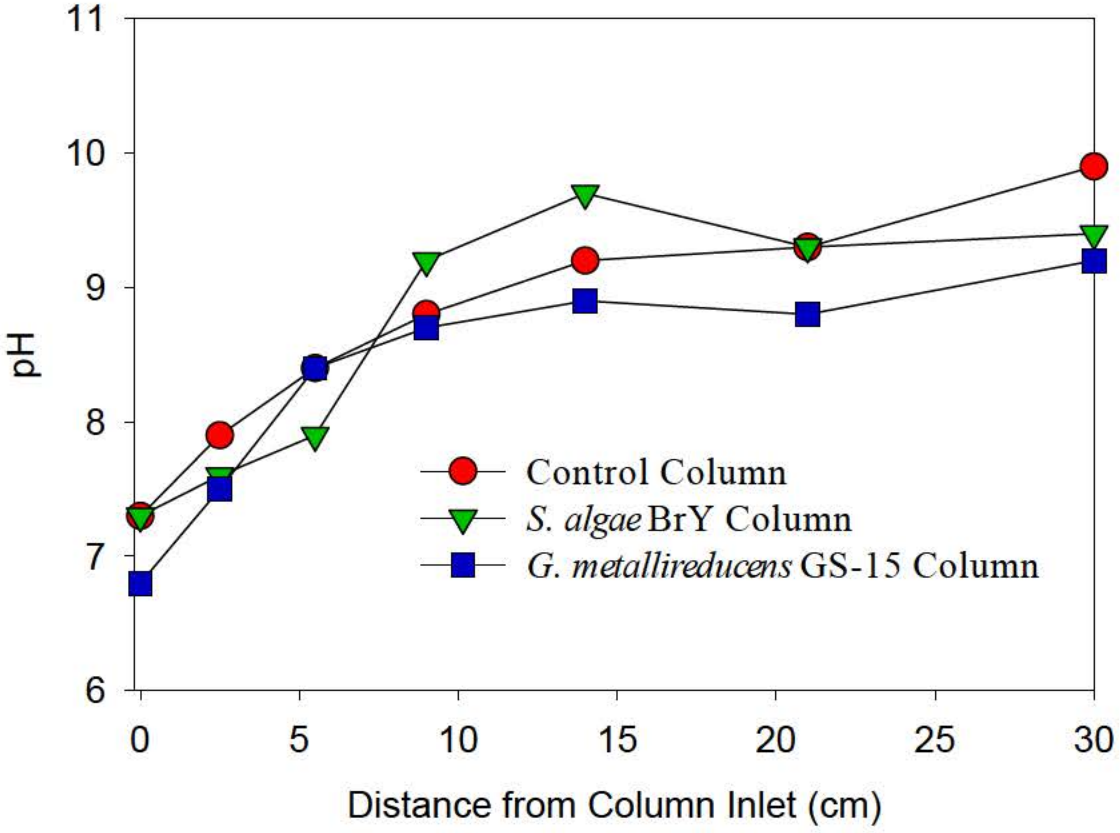

Fig. 14. pH profile for flow-through Fe(0) columns

The Mössbauer spectra from each sample (Figures 15-20) show a prominent doublet that can be identified as siderite ($FeCO_3$, CS=1.11, QSD=1.93 (McCammon, 1995)). Siderite is likely to form because a high concentration of bicarbonate (2 mM) exists in the column feed solutions. The spectra from each of the column's Fe^0 filings inlet are similar (Figure 15) and contain about the same percentage of siderite (about 60%). Siderite has been identified in Fe0 PRBs and in column studies with granular Fe0 (Mackenzie, et al., 1999; Phillips et al., 2000; Roh, et al., 2000) and has been shown to inhibit the reduction of nitrobenzene in batch reactors with granular Fe0 (Agrawal, et al., 1996). The percentage of siderite, however, decreased at the outlet of the Fe0 filings in the *G. metallireducens* column, possibly due to reaction with RDX, dissolution, or simply heterogeneities in the column.

Samples analyzed from three zones within GS-15 bioaugmented column (Figures 17-19) Fe^0 filings inlet, Fe^0 filings outlet, downgradient sand) show a decrease in relative abundance of siderite (from 67% to 26%, Table 8). It is likely that the chemical composition of the column feed solution partially governs the identity of precipitated iron minerals. High concentrations of bicarbonate at the Fe^0 filings inlet provide favorable conditions for siderite formation, which diminishes downgradient presumably as more bicarbonate becomes sequestered within precipitates or consumed by microorganisms. The spectrum of the downgradient sand shows a small but discernable amount of siderite as well as an unidentified component that resembles a mixed-valent iron species. A magnetic sextet is also present within the downgradient sand spectrum.

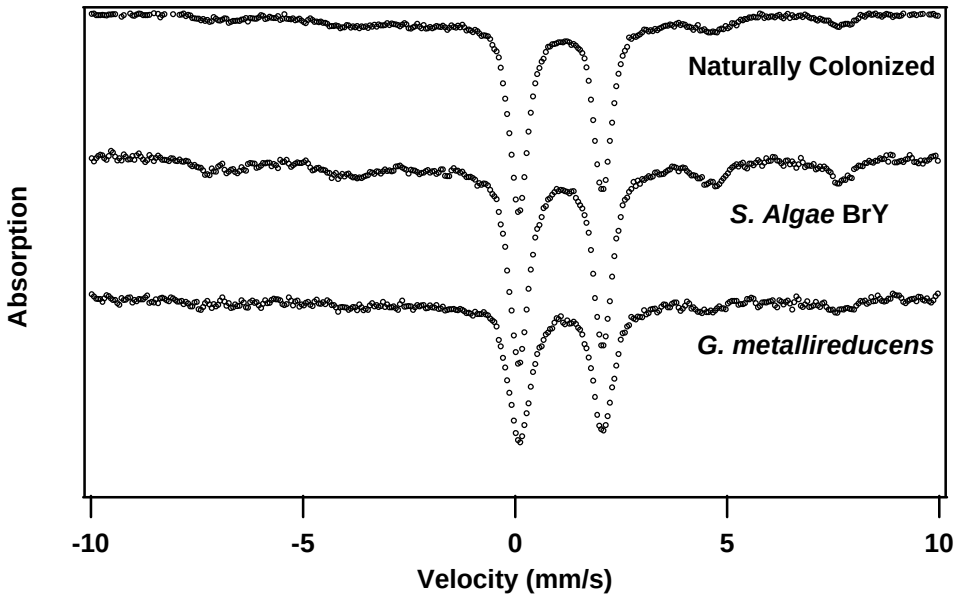

Fig. 15. Comparison of Mössbauer spectra for solid samples from the inlet of each column.

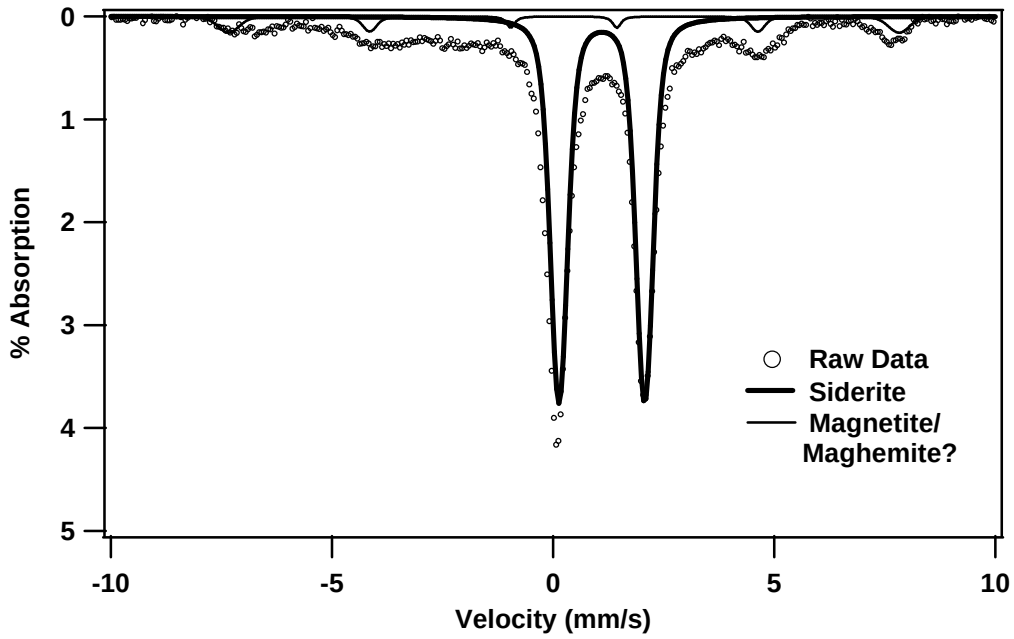

Fig. 16. Mössbauer spectra for Fe^0 filings inlet of naturally colonized (indigenous) column

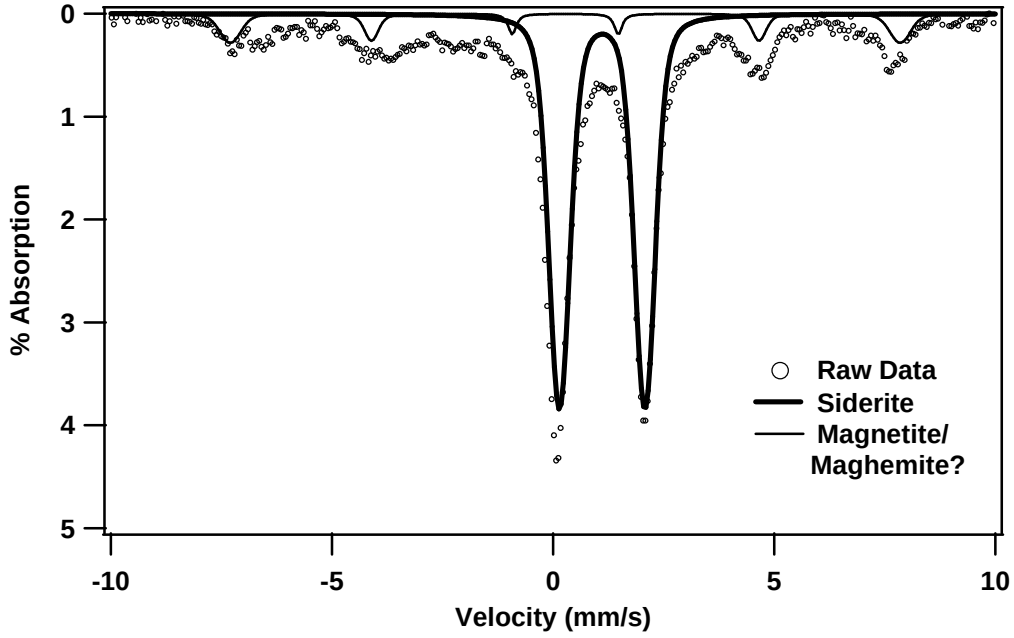

Fig. 17. Mössbauer spectra for Fe^0 filings inlet of column bioagumented with *S. algae BrY*.

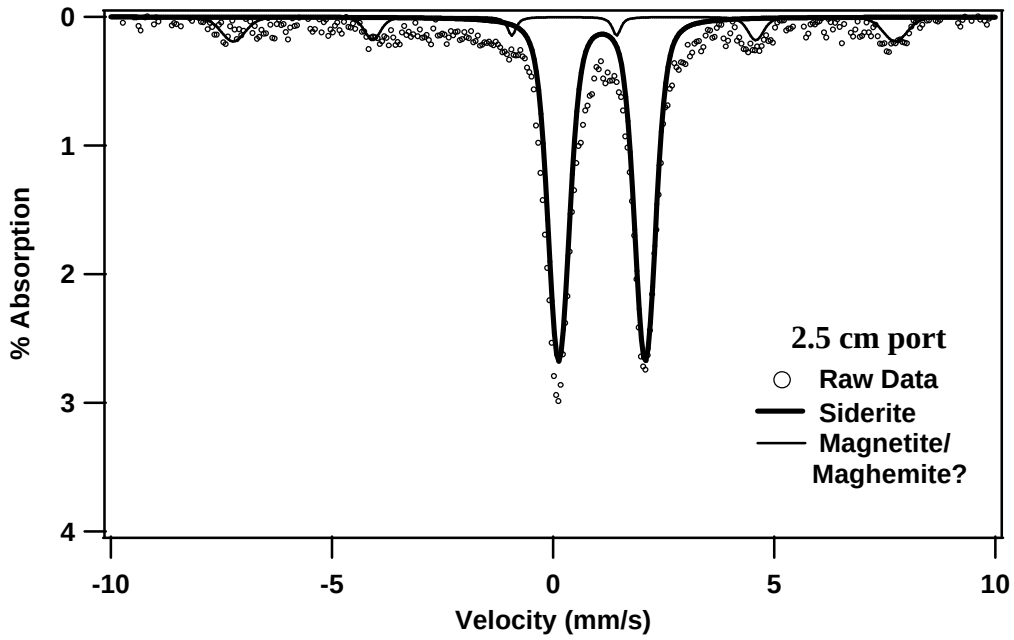

Fig. 18. Mössbauer spectra for Fe^0 filings inlet of column bioagumented with *G. metallireducens* GS-15.

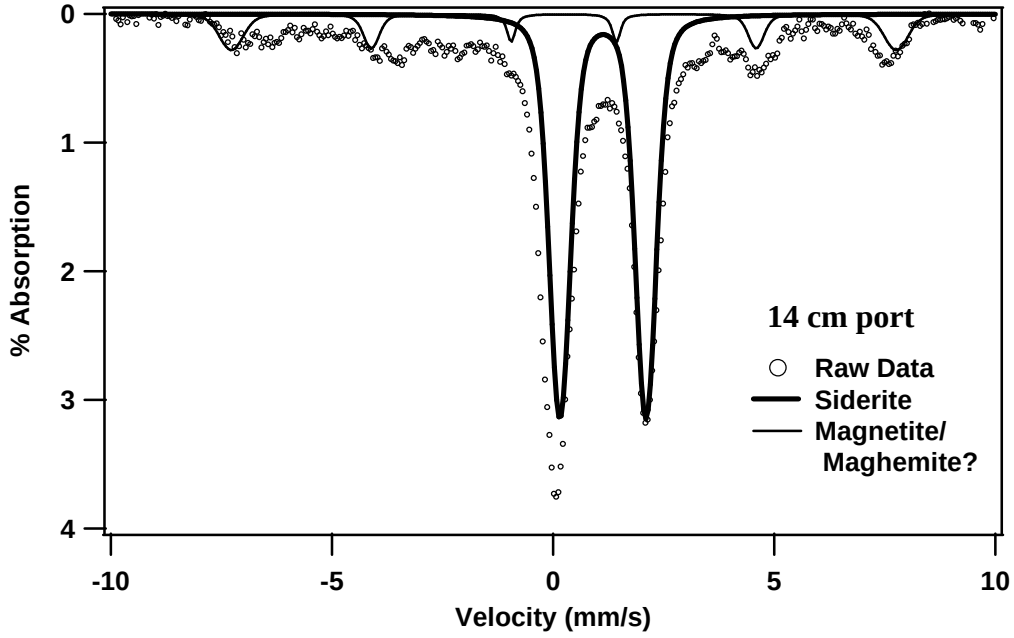

Fig. 19. Mössbauer spectra for Fe^0 filings (14 cm from inlet) of column bioagumented with *G. metallireducens* GS-15.

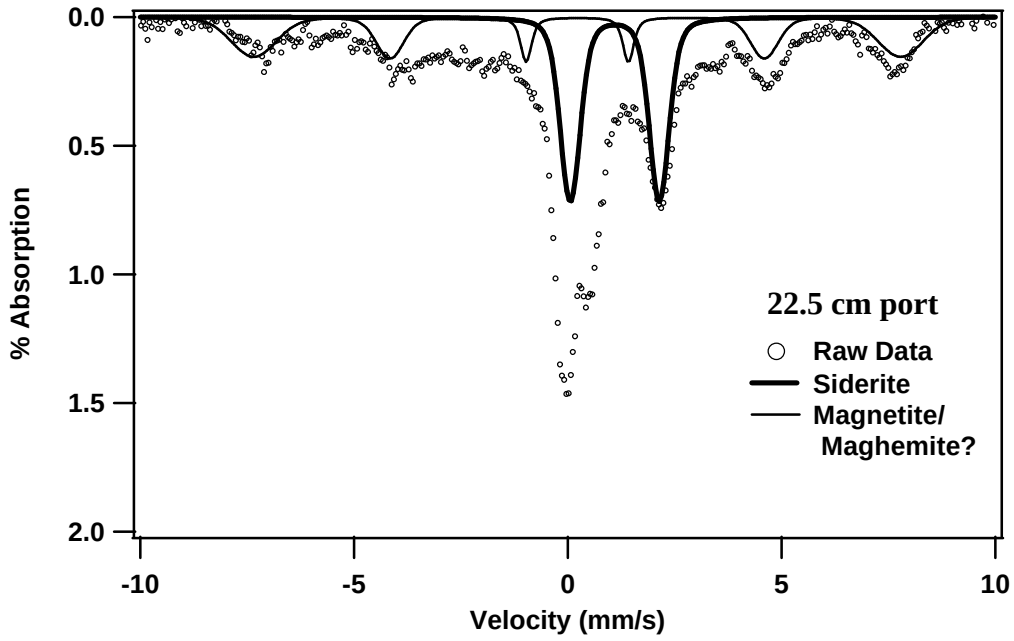

Fig. 20. Mössbauer spectra for downgradient sand zone (22.5 cm from inlet) of column bioagumented with *G. metallireducens* GS-15.

Table 8: Measured Mössbauer parameters for solid samples from Aged-Iron Columns.

			Mössbauer Parameters					
			Measured			Ref: McCammon (1995)		
Column Sample	Mineral	Percent Abundance	CS* mm s^{-1}	*QSD** mm s^{-1}	H* Tesla	CS* mm s^{-1}	*QSD** mm s^{-1}	H* Tesla
Naturally colonized, Fe^0 filings inlet (2.5 cm)	**Dominant Phase**							
	siderite	59%	1.10	1.93	--	1.24	1.80	--
	Detected Phases							
	vivianite		1.18	3.08	--	1.21	2.98	--
			1.13	2.63	--	1.18	2.45	--
			0.40	1.09	--	0.38	1.06	--
			0.33	0.74	--	0.40	0.61	--
	magnetite		0.24	--	47.0	0.26	--	49.0
			0.61	--	44.0	0.67	--	46.0
	Fe^0		0.00	--	31.4	0.00	--	33.0
	maghemite		0.30	--	44	0.32	--	45-52
S. algae BrY Fe^0 filings inlet (2.5 cm)	**Dominant Phase**							
	siderite	56%	1.11	1.93	--	1.24	1.80	--
	Detected Phases							
	vivianite		1.21	3.00	--	1.21	2.98	--
			1.18	2.50	--	1.18	2.45	--
			0.38	1.07	--	0.38	1.06	--
			0.4	0.68	--	0.40	0.61	--
	magnetite		0.27	--	46.9	0.26	--	49.0
			0.59	--	44.5	0.67	--	46.0
	Fe^0		0.00	--	31.0	0.00	--	33.0
	maghemite		0.31	--	43.0	0.32	--	45-52
G. metallireducens, Fe^0 filings inlet (2.5 cm)	**Dominant Phase**							
	siderite	67%	1.11	1.93	--	1.24	1.80	--
	Detected Phases							
	vivianite		1.21	3.00	--	1.21	2.98	--
			1.18	2.50	--	1.18	2.45	--
			0.38	1.07	--	0.38	1.06	--
			0.4	0.68	--	0.40	0.61	--
	magnetite		0.27	--	46.9	0.26	--	49.0
			0.59	--	44.5	0.67	--	46.0
G. metallireducens, Fe^0 filings outlet (14 cm)	**Dominant Phase**							
	siderite	51%	1.13	1.95	--	1.24	1.80	--
	Detected Phases							
	vivianite		1.20	3.00	--	1.21	2.98	--
			1.21	2.55	--	1.18	2.45	--
			0.38	1.11	--	0.38	1.06	--
			0.35	0.61	--	0.40	0.61	--
	magnetite		0.24	--	46.6	0.26	--	49.0
			0.58	--	44.2	0.67	--	46.0
	Fe^0		0.00		33.4	0.00	--	33.0
G. metallireducens, Sand zone (22.5 cm)	**Detected Phases**							
	siderite		1.13	1.95	--	1.24	1.80	--
	unknown mixed valent phases							
	magnetite		0.24	--	46.6	0.26	--	49.0
			0.58	--	44.2	0.67	--	46.0

* CS = Center Shift, QSD = Quadruple Splitting Distribution, H = Magnetic Splitting.

Batch Microcosm Studies

Biological Removal of RDX using selected pure cultures of *Acetobacterium*

Background

In past reports, we showed that iron samples from both the colonized and bioaugmented columns contained high proportions of *Acetobacterium* sp. (Oh and Alvarez, 2002), which are strict anaerobes that use H_2 and CO_2 for growth and produce acetate:

$$4H_2 + 2CO_2 \rightarrow CH_3COO^- + H^+ + 2H_2O \qquad \text{(Eq. 1)}$$

Note that H_2 could be provided by the anaerobic corrosion of iron with water:

$$Fe^0 + 2H_2O \rightarrow H_2 + Fe^{+2} + 2OH^- \qquad \text{(Eq. 2)}$$

In theory, such homoacetogens could comensalistically support heterotrophic activity in Fe^0 barriers by coupling Fe^0 corrosion (Equation 2) with acetogenesis (Equation 1):

$$4Fe^0 + 2CO_2 + 5H_2O \rightarrow CH_3COO^- + 4Fe^{+2} + 7OH^- \qquad \text{(Eq. 3)}$$

These results are supported by previous reports that the homoacetogen, *Acetobacterium woodi,* can grow on cathodic hydrogen from iron corrosion (Rajagopal and LeGall, 1989). Increased availability of an organic substrate (i.e., acetate) is likely to increase heterotrophic activity, which might be beneficial for RDX biodegradation, especially if RDX is utilized as a nitrogen source by heterotrophs (Sheremata and Hawari, 2000). Homoacetogens have also been implicated in RDX degradation by methanogenic sludge (Adrian and Lowder, 1999). Nevertheless, the ability of homoacetogens to degrade RDX under autotrophic (H_2-fed) conditions that are likely to be encountered in Fe^0 barriers has not been demonstrated.

The homoacetogenic bacteria *Acetobacterium paludosum* (ATCC# 51793) was studied for its ability to utilize RDX for growth. *A. paludosum* is a non-pathogenic, Gram-positive, strict anaerobe capable of growing both autotrophically or chemoorganotrophically with morphology

described as short nonspore-forming rods that are mobile by means of flagella. The optimal growth temperature for this strain is 20°C. The culture was obtained from American Type Culture Collection (ATCC, Manassas, VA).

Our hypothesis was that the rate and extent of RDX degradation would be increased when the bacteria are substrate-challenged. We sought to determine if these bacteria are capable of using RDX as a carbon or nitrogen source, or if they degrade RDX only by fortuitous cometabolism. Experiments were conducted where *A. paludosum* was grown and monitored under varying nitrogen- and carbon-containing conditions to see if the rate and extent of RDX biodegradation by these bacteria would be significantly affected by the availability of alternative substrates. Organic carbon sources, nitrogen sources, or both, were omitted from some treatments to test our hypothesis that RDX degradation might be faster under nutrient-limited conditions, which would exert selective pressure for the utilization of RDX as a nitrogen or carbon source.

Materials and Methods

For these experiments, the culture was grown on ATCC *Acetobacterium* medium 1019 (Balch and Wolfe, 1976) which contains the following (in grams per liter of distilled water): yeast extract (1.0); NH_4Cl (1.0); $MgSO_4 \cdot 7H_2O$ (0.1); KH_2PO_4 (0.4); K_2HPO_4 (0.4); fructose (5.0); $NaHCO_3$ (3.0); cysteine $HCl \cdot H_2O$ (0.5); and $Na_2S \cdot 9H_2O$ (0.5). The medium also contained Wolfe's Vitamin solution (10 mL), Wolfe's Mineral solution (10 mL), and resazurin (0.01%) as a redox potential indicator; the headspace consisted of a H_2/CO_2 mixture (95/5, v/v). In an effort to determine RDX biodegradation under different substrate conditions, assays were conducted in 25-mL Balch anaerobic culture tubes (18 × 150 mm) amended with 6 mL of autoclaved ATCC

1019 *Acetobacterium* medium, 1.5 mL of liquid cell culture, and RDX (approx. 3 mg/L). The headspace consisted of 20 mL of an H_2/CO_2 (80/20, v/v) gas mixture. We also investigated the growth of *A. paludosum* using RDX as the sole source of nitrogen. These tubes were prepared with RDX, 1.5 mL of bacteria, 6 mL of ATCC 1019 medium without an organic carbon source, and a headspace of H_2/N_2 (CO_2 was omitted). Controls without bacteria and controls in which the bacteria were unfed (no organic carbon or CO_2) were also prepared to obtain a baseline for comparing RDX degradation and acetate production. The tubes were covered in aluminum foil to prevent photo-interactions, and were rotated continuously on a Roto-Torque Heavy Duty Rotator (Cole-Palmer) at room temperature (approximately 20 °C). The optical density of each tube was recorded throughout the experiment to determine the viability of the bacteria. Table 9 shows the setup of the five total sets of treatments. The first four sets of tubes listed in Table 9 (the three biotic sets under different substrate conditions and the abiotic set) were prepared and started before the fifth control set, in which the only potential carbon source was RDX, was started a few days later.

Table 9. Experimental design to study RDX degradation by *A. paludosum* under different substrate conditions

Treatment	No. of replicates	Modification to medium	RDX, mg/L	Amount of cell culture	Headspace (v/v)
With NH_4^+ + CO_2 + H_2	4	Organic carbon substrates (fructose) omitted	2.75 ± 0.18	1.5 mL of culture with OD_{660} of 0.914	20 mL of 80/20 H_2/CO_2
With CO_2 + H_2 alone	3	Organic carbon substrates (fructose) omitted; ammonium chloride omitted	2.00 ± 0.13	1.5 mL of culture with OD_{660} of 0.914	20 mL of 80/20 H_2/CO_2
With organic C + NH_4^+ + CO_2 + H_2	3	No modification	3.31 ± 0.08	1.5 mL of culture with OD_{660} of 0.914	20 mL of 80/20 H_2/CO_2
Abiotic - organic C + NH_4^+ + CO_2 + H_2 but no bacteria	2	No modification – complete 1019 recipe	4.34 ± 0.18	None	20 mL of 80/20 H_2/CO_2
With NH_4^+ + H_2	3	Organic carbon substrates (fructose) omitted	3.54	1.5 mL of culture with OD_{660} of 0.718	H_2/N_2 mixture(approx. 5/95)

Results and Discussion

Table 10 summarizes the first three days of the experiment. In this initial part of the experiment, only initial and final samples were taken. All RDX was consumed in these treatments after three days of incubation. Loss of RDX in the abiotic control cannot be adequately explained, however, RDX removed in this control set was significantly less than observed in treatments with microorganisms.

Table 10. RDX degradation by *A. paludosum* after initial addition of RDX

Treatment	RDX Concentration, mg/L	
	Day 0	Day 3
With NH_4^+ + CO_2 + H_2	2.75 ± 0.18	ND
With CO_2 + H_2 alone	2.00 ± 0.13	ND
With organic C + NH_4^+ + CO_2 + H_2	3.31 ± 0.08	ND
Abiotic - organic C + NH_4^+ + CO_2 + H_2 but no bacteria	3.54	2.88

Treatments containing RDX as the sole carbon source to support growth of *A. paludosum* were examined for nine days, and approximately 62.3% of the initial RDX was degraded during that time. Data are presented in Table 11. The ability to degrade RDX without an additional carbon source present suggests that these bacteria may be using the RDX as a carbon source. However, as these bacteria were grown heterotrophically, they may have still contained an internal storage of carbon when they were added to these assays. We are planning to conduct experiments to more clearly determine what metabolic advantage if any is gained when these bacteria degrade RDX.

Table 11. RDX degradation by *A. paludosum* after initial addition of RDX, 2nd experimental control setup

Treatment	**RDX Concentration, mg/L**		
	Day 0	Day 9	% Removal
With $NH_4^+ + H_2$	3.50 ± 0.28	1.32 ± 0.59	62.3%

To examine the transformation capacity of the bacteria to degrade RDX under different substrate conditions, and to determine some kinetic properties, treatments were respiked with RDX (1.5 mL of RDX solution, approximately 30 mg/L, was added to each tube). An approximation of cell mass was tracked by monitoring the optical density at 660 nm. Table 15 shows the initial RDX concentrations in the tubes after they were respiked with RDX and the RDX concentrations after 10 days of operation. Figure 21 shows a linearization of the first order reaction of the three treatments up to day 6. The RDX data were normalized by the average OD_{660} in order to account for differences in the concentration of bacteria in each tube. The linear treadlines fit the data well and show that initially (until day 6), the data follow a first-order reaction. Initial rate kinetic coefficients (i.e., first-order) were determined for these treatments and are summarized in Table 16.

Table 15. RDX degradation by *A. paludosum* after 2nd addition of RDX

Treatment	RDX Concentration, mg/L		
	Day 0	Day 10	% Removal
With $NH_4^+ + CO_2 + H_2$	9.25 ± 0.31	0.38 ± 0.39	95.9%
With $CO_2 + H_2$ alone	7.80 ± 0.16	0.05 ± 0.08	99.4%
With organic C + NH_4^+ + $CO_2 + H_2$	9.07 ± 0.6	2.50 ± 0.23	72.4%
Abiotic - organic C + NH_4^+ + CO_2 + H_2 but no bacteria	14.24	13.59	4.6%
With $NH_4^+ + H_2$	9.01 ± 0.49	5.88 ± 1.69	34.7%

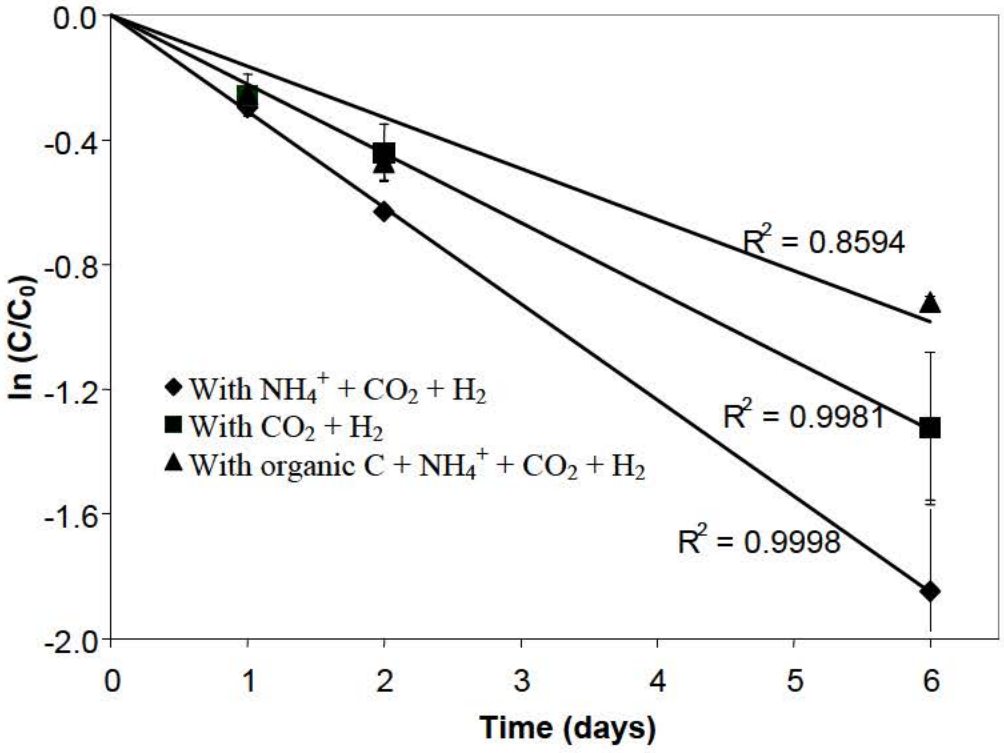

Fig 21. RDX removal by *A. paludosum* under different substrate conditions (second spike). Error bars represent 95% confidence intervals.

Even though the initial concentration of RDX was about 3 times higher than control treatments, the bacteria in medium with limited substrates (where either organic carbon or organic carbon and nitrogen sources were omitted) had the highest percentage of RDX degradation. The bacteria exposed to medium without an organic carbon source had a 95.9% decrease in RDX concentration in six days compared to a 99.4% decrease tubes containing medium without an organic carbon source or a nitrogen source ($p < 0.05$). There was no significant difference between these two substrate-limiting treatment types. However, they are statistically different from the controls and the assay amended with medium containing both an organic carbon source and a nitrogen source. The fact that these bacteria will degrade RDX faster when there is no nitrogen source other than RDX suggests that the absence of easily assimilated nitrogen sources, such as NH_4^+, can exert selective pressure on the bacteria to degrade RDX.

As seen in Figure 20, the rate of RDX biodegradation in the three treatment sets through day 6 closely followed first-order kinetics (i.e., $C = C_0e^{-kobs*t}$) and the data can be linearized according to Equation 4:

$$\ln (C/C_0) = -k_{obs}*t \qquad \text{(Eq. 4)}$$

where k_{obs} is the observed first order rate coefficient. C_0 and C are the initial and time *t* concentrations of RDX in solution. These rate coefficients, and their corresponding R^2 values, are summarized in Table 5 (normalized by initial OD_{660}). For this second addition of RDX, the k values are all significantly different from each other (statistically, by 95% confidence). The treatment tubes in which there was NH_4^+, CO_2, and H^+ degraded RDX the fastest, followed by

the tube sets in which RDX was the only potential nitrogen source. It is interesting to note that these two treatments, in which less easily assimilated carbon and nitrogen sources where present, had higher k values than the biotic treatment in which organic carbon and NH_4^+, both easily assimilated, are present.

Table 16. 1st order rate coefficients for the degradation of RDX by *A. paludosum* during the 2nd and 3rd additions of RDX , ± represent 95% confidence intervals

Treatment	**2nd addition of RDX**		**3rd addition of RDX**		**% diff.**
	1st order rate coefficient, k, $(days*OD_{660,0})^{-1}$	R^2 value	1st order rate coefficient, k, $(days*OD_{660,0})^{-1}$	R^2 value	
With NH_4^+ + CO_2 + H_2	1.75 ± 0.17	0.93	2.14 ± 0.43	0.89	22
With CO_2 + H_2 alone	1.29 ± 0.12	0.96	3.10 ± 0.28	0.97	140
With organic C + NH_4^+ + CO_2 + H_2	0.31 ± 0.04	0.92	1.03 ± 0.05	0.99	229

After 10 days, the three biologically active sets of tubes (not the controls) were spiked again with RDX (approx. 3 mg/L per tube) to determine if RDX would continue to be transformed. The initial and final RDX concentrations are presented in Table 17 and the calculated k values, assuming first-order kinetics, are presented in Table 16. During this period, the treatment in which RDX was the sole source of nitrogen degraded the RDX faster the other treatments. There was a statistically significant difference between all treatments. It is also interesting to note that the rates of degradation in the treatment without NH_4^+ and the treatment with NH_4^+ and organic carbon showed little change from the second to the third additions of RDX. However, the rate of degradation of the treatment containing NH_4^+ but no organic carbon decreased by about 50%. This could indicate a lower transformation capacity for autotrophic RDX degradation when NH_4^+ is present.

Table 17. RDX degradation by *A. paludosum* after 3rd addition of RDX

Treatment	**RDX Concentration, mg/L**		
	Day 0	Day 10	% Removal
With $NH_4^+ + CO_2 + H_2$	4.55 ± 0.20	0.50 ± 0.42	89.6%
With $CO_2 + H_2$ alone	4.35 ± 0.18	0.14 ± 0.08	96.9%
With organic C + $NH_4^+ + CO_2 + H_2$	5.76 ± 0.85	0.34 ± 0.11	93.5%

During the course of the experiment, acetate production and optical density was tracked. These data are summarized in Tables 18 and 19 and show that there is growth and acetate production in all treatments except in the abiotic controls and the tubes that contain only RDX as a potential source of carbon. The bacteria in the tubes that contained organic carbon and NH_4^+ (heterotrophic conditions) grew the most and produced the most acetate overall, as expected. Comparing the growth and acetate production after RDX was added the second and third times, much less activity after RDX was added the second time. This is most likely due to the fact that a much higher concentration of RDX was added the second time (~ 9 mg/L) than the third (~4.5 mg/L). This higher concentration probably inhibited cell growth and acetate production. After RDX was added a third time, the bacteria in the tubes without an alternative nitrogen source grew the most and produced the most acetate of the treatments. These data and the data contained in the tables above suggest that the absence of an easily assimilated nitrogen source (such as NH_4^+) can exert selective pressure on *A. paludosum* to use RDX as the sole source of nitrogen. Future experiments will be performed to further test our theory that *A. paludosum* can grow using RDX as a sole nitrogen source under autotrophic conditions (such as those that might be found in an iron barrier).

Table 18. Optical density (at 660 nm) of tubes containing *A. paludosum* under different substrate conditions, ± one standard deviation

	OD_{660}, 1st addition of RDX			OD_{660}, 2nd addition of RDX			OD_{660}, 3rd addition of RDX		
Treatment	Day 0	Day 3	% incr.	Day 0	Day 10	% incr.	Day 0	Day 21	% incr.
With $NH_4^+ + CO_2 + H_2$	0.19 ± 0.01	0.20 ± 0.02	5.3	0.18 ± 0.00	0.19 ± 0.01	5.6	0.07 ± 0.00	0.14 ± 0.03	100
With $CO_2 + H_2$ alone	0.19 ± 0.01	0.20 ± 0.02	5.3	0.17 ± 0.00	0.17 ± 0.01	0	0.07 ± 0.01	0.21 ± 0.02	200
With organic C + $NH_4^+ + CO_2 + H_2$	0.20 ± 0.01	0.61 ± 0.05	205	0.51 ± 0.04	0.48 ± 0.08	-5.9	0.18 ± 0.04	0.62 ± 0.11	244
With $NH_4^+ + H_2$	*	*	*	0.06 ± 0.03	0.04 ± 0.01	-33.3	*	*	*

Table 19. Acetate production (mmol) in tubes containing *A. paludosum* under different substrate conditions, ± one standard deviation

	Acetate (mmol), 1st addition of RDX			Acetate (mmol), 2nd addition of RDX			Acetate (mmol), 3rd addition of RDX		
Treatment	Day 0	Day 3	% incr.	Day 0	Day 10	% incr.	Day 0	Day 21	% incr.
With $NH_4^+ + CO_2 + H_2$	ND	5.92 ± 1.43	100	18.89 ± 1.36	25.59 ± 1.78	35.47	9.59 ± 0.75	27.51 ± 5.88	187
With $CO_2 + H_2$ alone	ND	7.47 ± 0.75	100	18.30 ± 1.14	22.26 ± 0.52	21.64	9.63 ± 0.37	41.85 ± 0.86	335
With organic C + $NH_4^+ + CO_2 + H_2$	ND	30.49 ± 0.92	100	33.29 ± 5.82	28.39 ± 6.34	-14.72	13.78 ± 2.28	65.61 ± 6.70	376
With $NH_4^+ + H_2$	*	*	*	ND	ND	0	*	*	*
Abiotic - organic C + $NH_4^+ + CO_2 + H_2$ but no bacteria	ND	ND	0	ND	ND	0	*	*	*

Note: In both Tables 18 and 19, ND = not detected and * = not tested

In an effort to understand if *A. paludosum* was able to use RDX as a source of nitrogen we investigated whether the presence of an easily assimilated nitrogen source, such as ammonium, would be inhibitory to RDX degradation. A significant decrease in RDX degradation in the presence of ammonium as compared to treatments in which RDX was the only possible nitrogen source would suggest that *A. paludosum* was using RDX as a nitrogen source. Nitrogen sources would be used preferentially, in the order of most biologically available to least. If this were the case, RDX would not be significantly degraded until the more easily assimilated nitrogen sources were exhausted.

Figure 22 shows the autotrophic degradation of RDX by *A. paludosum* under two nitrogen conditions: with and without ammonium (NH_4^+ added as NH_4Cl). The data were plotted and fitted with an exponential decay regression line. The first time RDX was spiked (as seen in the first pane of Figure 21) there was no statistically significant difference between the two treatments. The normalized (by the initial OD_{660}) rate of decay of the treatment containing NH_4^+ was 4.43 $(day*OD_{660})^{-1}$ while the normalized rate of decay of the treatment not containing NH_4^+ was 4.57 $(day*OD_{660})^{-1}$. The initial similarity of rates of decay possibly reflect that the cells contained internally sufficient reducing power and/or nitrogen sources. A second spike with RDX resulted in greater difference between the two treatments (Figure 21). The rate of exponential decay of the treatment without NH_4^+ increased slightly to 4.52 $(day*OD_{660,0})^{-1}$ while that of the treatment that contained NH_4^+ decreased by almost half, to 2.41 $(day*OD_{660,0})^{-1}$. The decrease in rate of degradation in the treatment containing a nitrogen source may be because the bacteria were running out of reducing power. The fact that the rate of degradation in the treatment without NH_4^+ remains near constant and still much greater

than that of the treatment containing NH_4^+ suggests that the RDX might have been serving as a nitrogen source for the bacteria, and that the presence of a more easily assimilated nitrogen source, such as NH_4^+ might inhibit RDX degradation.

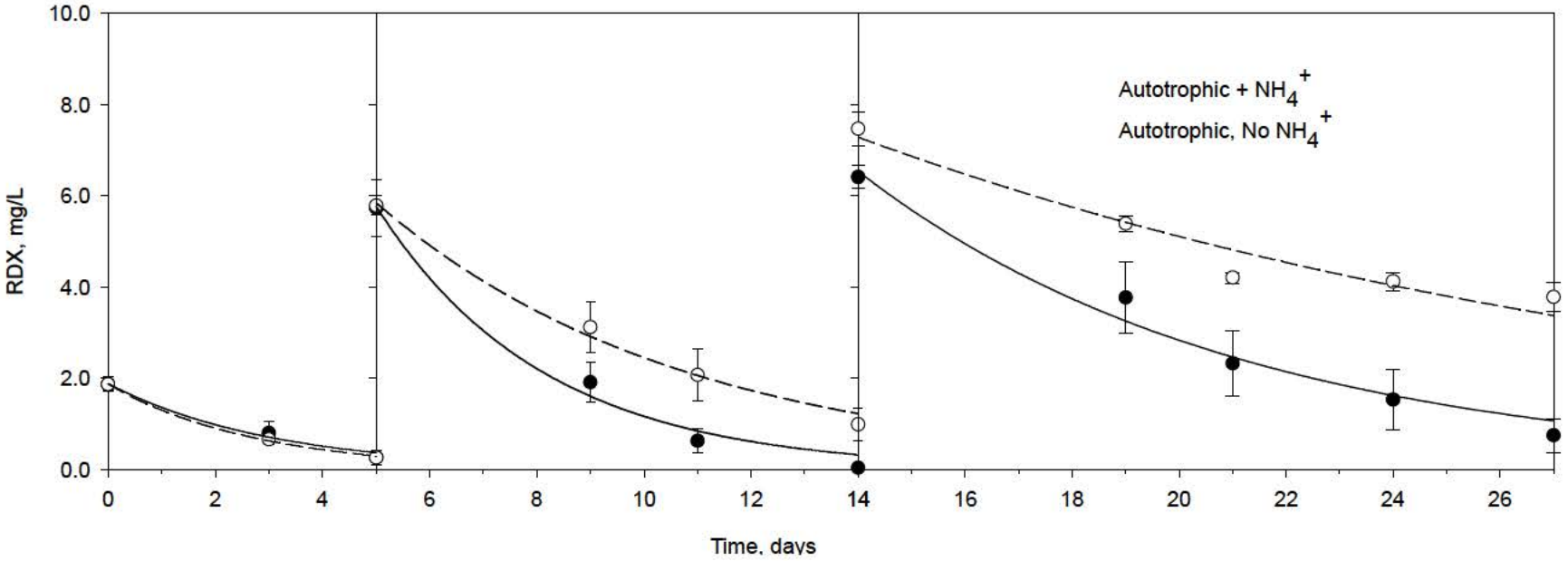

Fig. 22 RDX removal by *A. paludosum* under utotrophic, anaerobic conditions with and without the presence of ammonium, (first, second, and third spikes of RDX). Error bars represent 95% confidence intervals.

A third spike with RDX was performed to determine if this trend was reproducible. The last pane in Figure 21 shows a statistically significant difference between the two treatments, with the treatment without NH_4^+ again degrading RDX significantly faster than the treatment with NH_4^+. However, RDX degradation rates in both treatments decreased significantly from the second spike. Whether this might be due to an accumulation of an inhibitory metabolite was not be determined because this experiment was conducted with unlabeled RDX. The normalized rates of decay for all three spikes are presented in Table 20. Tables 21 and 22 show changes in optical density and acetate concentration in each treatment.

From these two experiments, it is still not clear why *A. paludosum* is able to degrade RDX. It does not appear that RDX is serving as a carbon source because no growth was observed in treatments with RDX as the sole source of carbon. These bacteria may degrade RDX by fortuitous cometabolism and utilize some of the products as nitrogen source.

Table 20: Normalized exponential decay rates for the degradation of RDX by *A. paludosum* with or without ammonium, ± 95% confidence intervals.

Treatment	1st spike of RDX	2nd spike of RDX	3rd spike of RDX
	Exponential decay rate, b, $(days*OD_{660,0})^{-1}$	Exponential decay rate, b, $(days*OD_{660,0})^{-1}$	Exponential decay rate, b, $(days*OD_{660,0})^{-1}$
Autotrophic, H_2 + CO_2 + NH_4^+	4.43 ± 0.71	4.52 ± 0.57	1.66 ± 0.12
Autotrophic, H_2 + CO_2 no NH_4^+	4.57 ± 0.30	2.41 ± 0.18	0.74 ± 0.13

Table 21: Optical density (at 660 nm) of tubes containing *A. paludosum* with or without ammonium, ± one standard deviation.

Treatment	OD_{660}, 1st addition of RDX			OD_{660}, 2nd addition of RDX			OD_{660}, 3rd addition of RDX		
	Day 0	Day 5	% incr.	Day 0	Day 9	% incr.	Day 0	Day 12	% incr.
Autotrophic, no NH_4^+, no RDX	0.077 ± 0.00	0.088 ± 0.00	14.29	0.075 ± 0.00	0.104 ± 0.00	38.00	0.089 ± 0.00	0.095 ± 0.00	6.78
Autotrophic + NH_4^+, no RDX	0.075 ± 0.00	0.097 ± 0.00	28.67	0.080 ± 0.00	0.121 ± 0.00	551.57	0.105 ± 0.00	0.125 ± 0.00	19.14
Autotrophic + NH_4^+	0.073 ± 0.003	0.085 ± 0.007	15.46	0.071 ± 0.005	0.111 ± 0.008	57.08	0.097 ± 0.007	0.104 ± 0.013	7.59
Autotrophic, no NH_4^+	0.080 ± 0.009	0.086 ± 0.009	6.88	0.071 ± 0.007	0.101 ± 0.012	39.79	0.087 ± 0.009	0.088 ± 0.012	1.44

Table 22: Acetate production (mmol) in tubes containing *A. paludosum* with or without ammonium, ± one standard deviation.

Treatment	Acetate (mmol), 1st addition of RDX			Acetate (mmol), 2nd addition of RDX			Acetate (mmol), 3rd addition of RDX		
	Day 0	Day 5	% incr.	Day 0	Day 9	% incr.	Day 0	Day 12	% incr.
Autotrophic, no NH_4^+, no RDX	1.29 ± 0.00	8.09 ± 0.00	524.72	6.49 ± 0.00	17.93 ± 0.00	176.93	14.97 ± 0.00	21.89 ± 0.00	46.18
Autotrophic + NH_4^+, no RDX	1.04 ± 0.00	9.31 ± 0.00	792.56	7.41 ± 0.00	19.17 ± 0.00	158.57	15.78 ± 0.00	26.63 ± 0.00	68.69
Autotrophic + NH_4^+	1.32 ± 0.41	7.27 ± 0.64	451.09	5.98 ± 0.65	17.54 ± 1.59	193.48	14.88 ± 1.00	22.61 ± 3.29	51.90
Autotrophic, no NH_4^+	2.29 ± 0.68	8.41 ± 0.92	267.98	7.04 ± 0.66	17.18 ± 3.72	143.96	14.57 ± 3.27	18.20 ± 2.76	24.90

Production of N_2O was observed in *A. paludosum* treatments amended with RDX. After one week incubation, cultures were monitored from days 7-14. Production of 0.003 mmol N_2O and 0.0009 mmol N_2O gas was measured in the treatments that degraded 0.00153 mmol (0.34 mg) RDX and 0.00149 mmol (0.33 mg) RDX, respectively. On a theoretical basis, where 3 moles of N_2O gas could possibly be generated from the 6 nitrogen atoms present in 1 mole RDX, an average of 0.0045 mmol could have been generated for the 0.00149-0.00153 mmol RDX degraded. Taking into account background measurements from non-RDX controls, the treatments produced 19-64% of theoretical N_2O possible. This upper value suggests that the nitrogen from the RDX heterocyclic ring was included in N_2O production suggesting ring-cleavage by *A. paludosum.* Results from these experiments are included in Table 23.

Table 23: Production of N2O by *A. paludosum* incubated with RDX

Treatment	RDX degraded	Maximum theoretical N_2O produced	Measured N_2O produced	Percentage of Theoretical Maximum N_2O produced*
With RDX 1	0.00153	0.00459	0.0030	64%
With RDX 2	0.00149	0.00447	0.0009	19%
Without RDX 1	NA	NA	0.0000	NA
Without RDX 2	NA	NA	0.00006	NA

NA-Not applicable
*Subtracting background from “Without RDX 2” Treatment

RDX Reduction by Iron Oxides

1. Reactivity of Sulfate Green Rust with RDX: Product Distribution

Background

The fate of RDX in the presence of sulfate green rust ($Fe^{II}_4Fe^{III}_2(OH)_{12}SO_4 \cdot yH_2O$) was further explored. We previously identified nitrous oxide (N_2O), methane (CH_4), and ammonium (NH_4^+) as preliminary end products. During this reporting period, a new gas-tight reactor was built to allow concurrent detection of products in the absence of a buffer. The evolution of N_2O and NH_4^+ was confirmed, the likelihood of CH_4 as a potential end product was eliminated, and the presence of formaldehyde (HCHO) was observed. In addition, ^{14}C-RDX was used to confirm that the majority of carbon products remain soluble and to better assess the fate of RDX in the presence of green rust.

Materials and Methods

The experiment and sample preparations were conducted within a glovebox under anoxic conditions. A batch reaction containing RDX (~370 uM), sulfate green rust (~6.0 g/L), and K_2SO_4 (16.7 mM, a background electrolyte) was performed within a gastight glass reactor vessel connected to a pH-stat and stir plate. Sulfate green rust was synthesized by induced hydrolysis of a combined FeII/FeIII solution (Williams and Scherer, 2001). A blue-green precipitate was recovered by vacuum-filtering and immediately added to the 120-ml reactor containing K_2SO_4. Freeze-drying the solids was not performed as in previous experiments. Solution pH was maintained at 7.0 using 0.25 N H_2SO_4 and 1.0 N KOH. The replacement of PIPES biological buffer (as was employed in previous experiments) with strong acid and base for pH maintenance permits the analysis of NH_4^+ without interference from PIPES.

The reactor was spiked with ^{12}C-RDX and approximately 4.0 uCi of uniformly labeled ^{14}C-RDX. Headspace and aqueous phase were sampled periodically. Concentrations of RDX and its nitroso transformation products were determined using HPLC-UV at 230 nm wavelenth (40/60 acetonitrile/ 1.0 g/L ammonium acetate mobile phase in a C-18 column) and a high-grade analytical standard (RDX) or synthesized laboratory standards (products). N_2O was measured using gas chromatography with an electron capture detector. NH_4^+ was analyzed using ion chromatography with auto suppression. HCHO was measured by first derivatizing with a 2,4-dinitrophenolhydrazine reagent (DNPH) in an acetate buffer agitated at 40 degrees C for one hour. The HCHO-DNPH derivative was analyzed using HPLC-UV at 360 nm (55/45 acetonitrile/ 1.0 g/L ammonium acetate mobile phase).

To assess whether any ^{14}C radioactivity had sorbed to the surface of green rust or its transformation solids, ^{14}C was extracted from samples containing the aqueous and solid phases by sonicating for one hour with acetonitrile. Samples containing only the aqueous phase were combined with acetonitrile and sonicated as well. Aliquots from both (i) the sonicated aqueous samples and (ii) the sonicated aqueous and solid phases samples were combined with Ultima-Gold scintillation cocktail and analyzed by liquid scintillation counting (LSC). ^{14}C radioactivity was also tracked using a radiochem detector connected in series to the HPLC-UV detector to correlate peaks containing ^{14}C radioactivity with UV-sensitive HPLC peaks.

Results and Discussion

The disappearance of 44 umoles of RDX within one hour in the presence of sulfate green rust results in the formation of HCHO, N_2O, and NH_4^+, which appear to be end products (Fig. 23). Trace MNX, DNX, and TNX were also detected within the first few minutes (data not

shown). Concurrent formation of NH_4^+, HCHO, and nitroso products suggests that RDX transformation occurs through rapid parallel pathways. A short time lag in N_2O formation was observed, suggesting N_2O formation might proceed through an intermediate transformation product. After two hours, approximately 58% of carbon from RDX were accounted for as HCHO, 22% of nitrogen as NH_4^+, and 22% of nitrogen as N_2O (for a total nitrogen balance of 44%).

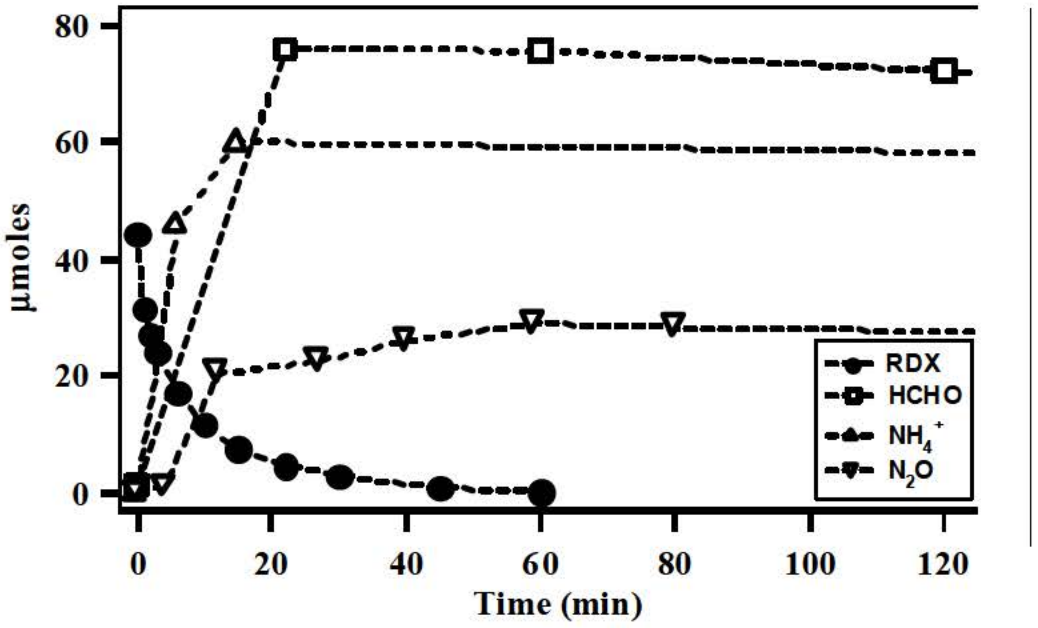

Fig. 23. Evolution of transformation products from RDX in the presence of sulfate green rust.

^{14}C radioactivity detected in samples using LSC show most carbon-containing products remaining in the aqueous phase (Table 24). Approximately 90% of ^{14}C radioactivity were recovered in the aqueous phase after 2 hours. No significant difference between ^{14}C radioactivity detected in samples containing either the aqueous phase or both the aqueous and solid phases reveals no significant amount of ^{14}C sorption to the solid phase. It is possible the unrecovered ^{14}C radioactivity partitioned to the gas phase as carbon-containing products not yet identified. We previously reported the formation of small amounts of methane in sealed reactor

vials containing PIPES buffer. No methane was detected, however, during this experiment. It is likely that methane was an artifact of the previous experiment. Future efforts will target identifying possible carbon-containing RDX transformation products (other than methane) in the reactor vessel headspace.

Table 24. Detected ^{14}C radioactivity (disintegration per minute) for the aqueous phase (aq) and both the aqueous and solid phase as extracted with acetonitrile (ext).

Time (min)	^{14}C dpm (aq)	^{14}C dpm (ext)
0	4400	--
60	3700	3800
120	3900	3800

Aqueous samples were also analyzed for ^{14}C radioactivity using a radiochem detector following HPLC-UV analysis. ^{14}C-RDX and some of its transformation products separated within the C-18 chromatography column appeared as peaks in the radiochem chromatogram. After 20 minutes, most of the ^{14}C radioactivity appears in the peak with a retention time of 2.9 minutes (Figure 24). A similar peak has been observed in microcosms containing RDX and pure cultures of homoacetogens as well as in reactor vials containing RDX and synthetic magnetite with dissolved Fe^{2+}. A smaller peak also occurs at 3.6 minutes, followed by a peak at 8.2 minutes that corresponds to ^{14}C-RDX. After derivatization for HCHO analysis, most of the ^{14}C radioactivity shifted from 2.9 min to 6.0 min reflecting the HCHO-DNPH derivative (Figure 2). The shift suggests that most of the ^{14}C radioactivity in the original 2.9 min peak is HCHO. The RDX peak, the 3.6 min peak, and residual 2.9 min peak are still apparent after derivatization (a higher composition of acetonitrile in the eluent for derivatization was responsible for reduced retention times). Potential RDX transformation products present within the 3.6 min peak are currently being evaluated using LC/MS techniques.

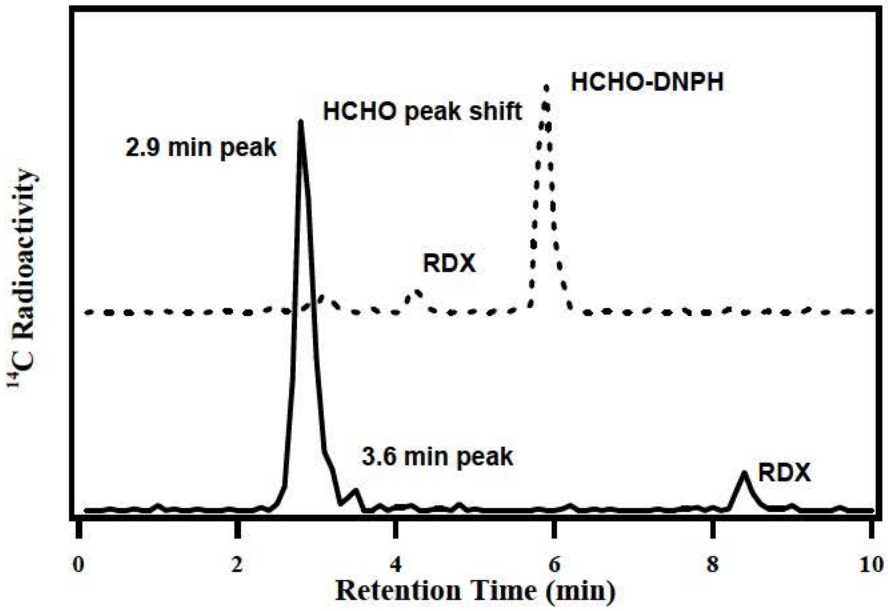

Fig. 24. Radiochem chromatograms for an aqueous sample taken at 20 minutes (solid line) and an aqueous sample at 20 minutes after DNPH derivatization for HCHO analysis (dashed line).

2. Reactivity of Carbonate Green Rust with RDX: Influence of Anions

Background

The reactivity of carbonate green rust ($Fe^{II}_4Fe^{III}_2(OH)_{12}CO_3 \cdot yH_2O$) with RDX was further explored. We previously reported rapid kinetics of RDX transformation in the presence of either sulfate or carbonate green rust. During this reporting period, we monitored the influence of common groundwater solutes (carbonate, sulfate, and phosphate) on the rate of reaction relative to the influence of bromide, which served as a background electrolyte for batch reactors. In addition, X-ray diffraction (XRD) was used to observe green rust transformation products. XRD is capable of distinguishing between different interlayer anions (e.g. carbonate or sulfate) and detecting possible surface precipitates that may form. Understanding how green rusts transform under different water chemistries is important for predicting their reactivity in groundwater environments.

Materials and Methods

The experiment and sample preparations were conducted within a glovebox under anoxic conditions. Four batch reactors, each containing RDX (~100 uM), carbonate green rust (4.0 g/L), and a background electrolyte solution with ionic strength of 0.1M were set up to evaluate the effect of commonly occurring groundwater anions. Bromide was selected as the reference anion, and the first reactor contained 0.1 M KBr. Subsequent reactors contained 10 mM of either $KHCO_3$, K_2SO_4, or KH_2PO_4 and enough KBr to poise the ionic strength at 0.1M. Carbonate green rust was synthesized by induced hydrolysis of a combined Fe^{II}/Fe^{III} solution (Williams and Scherer, 2001). A blue-green precipitate was recovered by vacuum-filtering and immediately freeze-dried. Solution pH was maintained at 7.0 using 1.0 M HBr and 1.0 M KOH.

The aqueous phase was sampled periodically for two hours. Concentrations of RDX were determined using HPLC-UV at 230 nm wavelenth (40/60 acetonitrile/ 1.0 g/L ammonium acetate mobile phase in a C-18 column) and a high-grade analytical standard. After two hours, the solids were filtered and preserved with glycerol for immediate XRD analysis. A sample of freeze-dried carbonate green rust was also prepared for XRD analysis.

Results and Discussion

In the presence of carbonate green rust, RDX is rapidly removed from solution when bromide is the sole anion electrolyte (Figure 25). As previously reported, the reaction rate follows pseudo-first order kinetics. The presence of 10 mM of sulfate or carbonate results in significantly slower RDX removal. When sulfate or carbonate is present, the reaction kinetics deviate from pseudo-first order, which suggests an unidentified surface reaction is participating. Phosphate has a more dramatic effect with no RDX removal observed over a period of 2 hours.

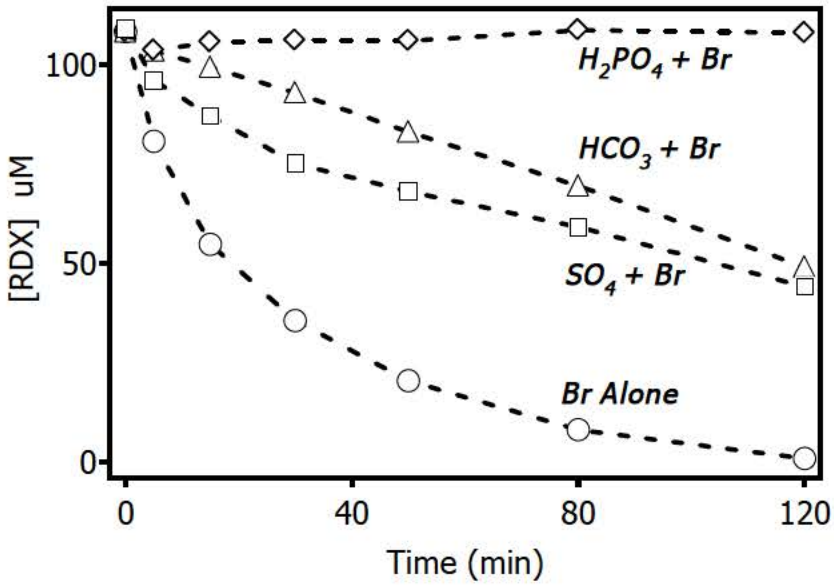

Fig. 25. Disappearance of RDX from solution in presence of 4.0 g/L carbonate green rust and common groundwater anions.

We hypothesize that the anions may interfere with the transformation of RDX by green rusts by (1) precipitating and forming a passivating surface coating (e.g., siderite, $FeCO_3$, or vivianite, $Fe_3(PO_4)_2$), (2) exchanging with carbonate within the green rust interlayer, or (3) complexing at the green rust surface. To help distinguish among these processes, we made XRD measurements, which can reveal the presence of surface precipitates or exchange of interlayer anion, but cannot observe the anions if they are complexed at the surface. For the reactor containing only bromide as the anion, the XRD spectrum reveals no green rust transformation solids after two hours (Figure 26). Minor amounts of Fe^{III}-containing solids may have formed due to oxidation of Fe^{II} by RDX but are not detected by XRD. Nevertheless, a predominating carbonate green rust signal is expected because green rust is in excess within the reactors.

Similarly, for the reactor containing bromide and bicarbonate, only carbonate green rust was detected. In contrast, the XRD spectra of the solid phases formed in reactors containing

either sulfate or phosphate reveal the presence of mineral phases other than carbonate green rust. In addition to carbonate green rust, sulfate green rust was observed in the presence of sulfate, and vivianite was detected in the presence of phosphate. The formation of additional mineral phases may be responsible for the observed decrease in reaction rate. Subsequent experiments may address solute interactions at the iron solid – water interface in order to better understand how green rust surfaces transform under environmental conditions.

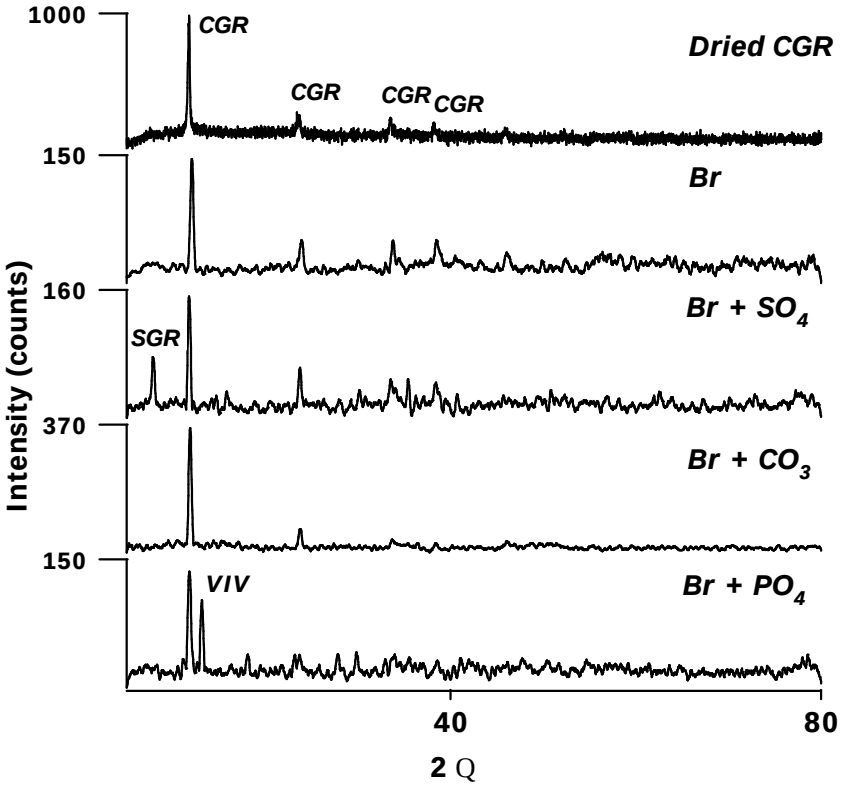

Fig. 26. XRD spectra of carbonate green rust solids after two hours exposure to RDX and different anions. A spectra of powder carbonate green rust is provided for reference. *CGR* = carbonate green rust; *SGR* = sulfate green rust; *VIV* = vivianite.

Metabolic Capabilities of Shewanella alga BrY: *RDX Utilization N Source*

Background

Last year, we reported that the facultative, iron(III)-reducing bacterium *Shewanella alga* BrY can degrade RDX, in both the presence and absence of ferric iron. Unlike other genera of iron reducers (e.g., *Geobacter*), *Shewanella* are tolerant to (and respire) oxygen, making them more adaptable to fluctuating environmental conditions. However, it is important to investigate how groundwater conditions inhibit or enhance this microbe's ability to utilize RDX. Since it is known that BrY cannot mineralize RDX, it is of interest to know just what metabolic niche RDX fulfills. For instance, if RDX is utilized as a nitrogen source, the presence of a preferential source like nitrate or ammonia might inhibit the rate at which BrY can degrade RDX.

Materials and Methods

Batch experiments were conducted to determine the ability of BrY to utilize different nitrogen sources during growth on lactate. Along with a batch containing RDX as the sole nitrogen source, replicate treatments were amended with either NH_4^+, NO_3^-, or N_2(g). The aim was to determine which nitrogen source best supported BrY growth, and thus which N sources might be preferentially utilized and inhibit the use of RDX as a nitrogen. A control with BrY without a nitrogen source was also prepared.

Mineral Medium Preparation. The growth medium contained (in g/L): 0.1 KCl, 0.5 K_2HPO_4, 10 NaCl, and 7.57 PIPES biological buffer. The pH of the buffered medium was adjusted to 7.0 with NaOH. Equal amounts of lactate (33 mM), Wolfe's mineral solution, and Wolfe's vitamin solution were added to each batch to fulfill nutrient requirements. Identical levels of nitrogen were provided in each batch. It was assumed that the three nitrogen atoms

from the nitro groups in RDX would be more readily available than RDX-ring nitrogen, so that 3 moles of N could be readily available to BrY per mole of RDX. All of the 125-mL serum bottles were sealed with blue septa and aluminum crimps. The batch containing N_2 as the sole nitrogen source was then purged with an 80%N_2/20%CO_2 gas mixture for 30 minutes. All other batches were purged with an 80%Ar/20%CO_2 gas mixture for 30 minutes to remove atmospheric nitrogen gas that could serve as a potential nitrogen source. The fact that *Shewanella oneidensis* MR-1, a similar strain, cannot fix nitrogen suggests that it is unlikely *S. alga* BrY would have this ability. Growth experiments were conducted under aerobic conditions to induce faster growth and obtain higher cell yields, which facilitate the evaluation of alternative N sources. Thus, after the batches were purged, 15 mg/L H_2O_2 was added to provide O_2 as an electron acceptor. Using McCarty stoichimetry, it was determined that the required RDX concentration to provide a sufficient amount of nitrogen to support significant growth would be above the solubility limit of RDX, and well above the toxic limit for BrY (McCarty, 1975). For this reason, RDX was periodically respiked multiple times to provide enough nitrogen (and avoid inhibition by high RDX concentrations) to support noticeable growth. Each time RDX was completely degraded in the batch, a respike of RDX was administered to achieve approximately 4 ppm RDX in the batch. This respike was needed approximately every seven (7) days.

Bacteria Preparation. *Shewanella algae* BrY was grown aerobically in 200 mL of tryptic soy broth (30 g/L, Difco Laboratories) at 30 °C on a rotary shaker at 150 rpm for 15 h. *S. algae* BrY cells were harvested during exponential growth phase by centrifugation, and cells were rinsed three times in a solution of 0.01 M PIPES biological buffer to remove residual TSB medium. Approximately 100 µl of rinsed bacterial suspension was added to each treatment.

Analytical Method. Growth-induced increases in optical density were monitored spectrophotometrically at a wavelength of 600 nm in a spectrophotometer. Also, as previously mentioned, RDX levels were monitored in the RDX batch to determine when to respike RDX without reaching inhibitory levels (ca. 5 mg/L). All reactors were stored at 30 °C on a rotary shaker at 150 rpm.

Table 25. Description of Microcosms

Treatment	Nitrogen Source
1	No nitrogen source provided (control)
2	RDX ($C_3H_6N_6O_6$)
3	Nitrate (NO_3^-)
4	Ammonia (NH_4^+)
5	Nitrogen gas (N_2)

Results and Discussion

Collected data from this experiment did little more than lead to further questions concerning the metabolic capabilities of *S. alga* BrY. Statistically significant growth was shown in all batches. The growth data can be seen below, in figure 27.

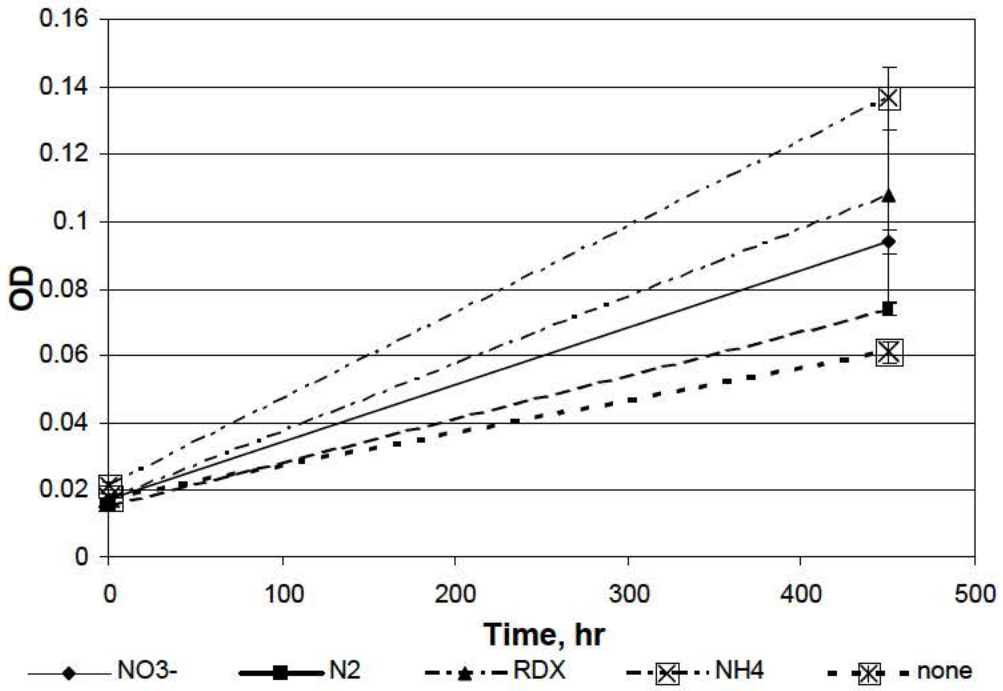

Fig 27. *Shewanella alga* BrY growth under different nitrogen conditions

These data were counterintuitive because growth occured in controls without nitrogen salts or RDX (e.g., treatments with N_2 in the headspace or no N source added). Apparently, the PIPES biological buffer ($C_8H_{18}N_2O_6S_2$) served as a nitrogen source. Usually this buffer is used in biological studies due to the fact that it is considered inert and microbes typically lack the ability to utilize it as a nutrient source. However, deductive elimination suggests that BrY used it as N source, which deserves communication to the scientific community. Nevertheless, this experiment was inconclusive. Due to the slow growth of BrY on RDX, it was not possible to further evaluate the possible growth of BrY under different nitrogen conditions within the time constraints of this project.

In addition, $N_2O(g)$ levels in batch headspace were monitored by gas chromatography. This is important to monitor as presence of N_2O in the headspace of the RDX batch would

suggest RDX ring fision (Hawari et al 2001). However, the detection limit for the method used is approximately 40 μM which is above the expected concentration in the headspace of the batch. We plan to repeat this experiment with lower headspace volume in relation to the liquid, to enhance N_2O detection. Increasing RDX concentrations to increase N_2O production is not a viable option due to RDX toxicity above 5 ppm.

Integrated Iron PRB with Down Gradient Natural Attenuation

Background

In contaminant remediation, even if active treatment is initially needed, monitored natural attenuation may be used to complete the cleanup (MacDonald, 2000). Flow-through columns were started in July 2003 to evaluate the feasibility of an integrated PRB-natural attenuation approach to intercept and treat RDX plumes. Emphasis was placed on determining the efficacy of bacteria in soils down gradient of a permeable reactive iron barrier to mineralize byproducts of RDX that escape the PRB. It would be desirable to show that any byproducts or RDX reduction by Fe(0) could be completely mineralized by naturally present microbes in the soil, to demonstrate process robustness and obviate concerns about potential toxicity or recalcitrance of RDX degradation products that could break through the PRB.

Materials and Methods

Two sets of two columns (15-cm long, 1.0-cm ID) in series each were equipped with inlet and outlet sampling ports. The first column in each set was packed with a 14-cm layer of autoclaved sand followed by an 1-cm layer of Master Builder® Fe(0) filings (1.0-2.0 mm diameter sieved) in order to simulate a reactive (thin) iron barrier. The second column in each

set was packed with a 15-cm layer of soil collected on the campus of The University of Iowa. A set of controls was also constructed. The control included two columns (15-cm long, 1.0-cm ID) connected in series as described above. Both of these columns were packed with inert glass medium. Flow through the columns was maintained at 1.5 ml/hr, allowing for approximately 40 minutes of contact time in the iron portion of the first column and ten hours of time allowed for natural attenuation in the soil column. A schematic of the system and its components can be found in figure 3, below.

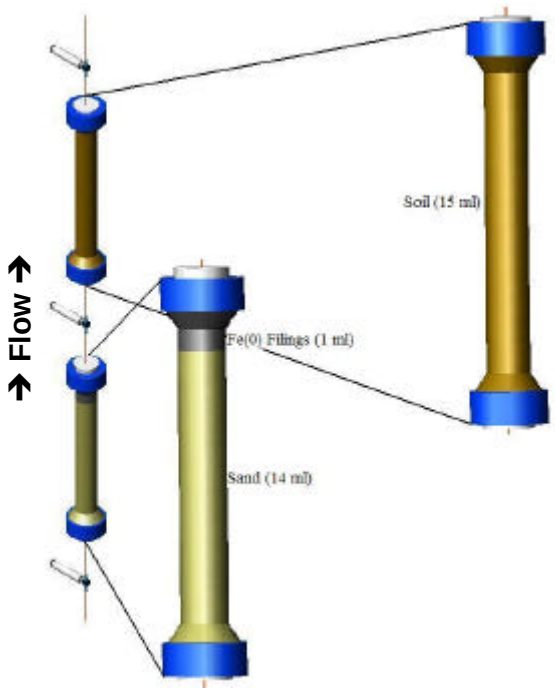

Fig. 28. Flow-through columns used to simulate permeable reactive iron barriers as well as the natural attenuation of byproducts that takes place downgradient of the PRB.

Iron and Sand Preparation. Iron filings were obtained from Master Builder® and sieved (1.0-2.0 mm diameter) to achieve homogeneity in this portion of the column. In order to pack the iron/sand column, water was first placed in the column to minimalize air pockets. The sand (14 ml) was then poured into the column and compressed. The iron filings (1 ml) were then added to

the top of the column and compressed as much as possible. These compression processes were included in order to prevent channeling in this first column.

Soil Preparation. Soil for use in these columns was collected from downtown Iowa City, IA. The soil was allowed to dry for a period of about two (2) days. The soil was then ground using a mortar and pestal and sieved to provide some homogeneity in the soil column. The soil was not sterilized to allow naturally occurring microbes to metabolize the RDX byproducts. In order to pack the soil column, water was first placed in the column to avoid air pockets. The soil was then poured into the column. The soil was not compressed as this would hinder free flow through the homogeneous particles.

Groundwater Medium Preparation. The synthetic groundwater medium used in this study contained (in mg/L): 41.4 $NaNO_3$, 272 K_2SO_4, 840 $NaHCO_3$, 16.3 NH_4Cl, 12.6 $MgCL_2?6H_2O$, 0.0087 $NaH_2PO_4?H_2O$, 0.0100 $Ni(NO_3)_2$, 0.0088 $ZnSO_4?$ H_2O, 0.0081 $CoCl_2?$ H_2O, 0.0034 MoO_3, 0.005 $CuSO_4$. In addition, this medium was amended with approximately 4 ppm RDX. All columns were allowed two (2) months to acclimate to a synthetic groundwater medium which was amended with approximately 4 ppm RDX. At this point, a spike of ^{14}C-RDX (30 µCi in 100 ml of media) was injected to determine the fate of RDX in the system.

Results and Discussion

The dissolved ^{14}C activity remained unchanged in the control column packed with inert glass beads (Fig. 4). This suggests that RDX was not transformed in the absence of Fe(0) or unsterile soil. Both columns containing Fe(0) removed RDX below detectable levels.

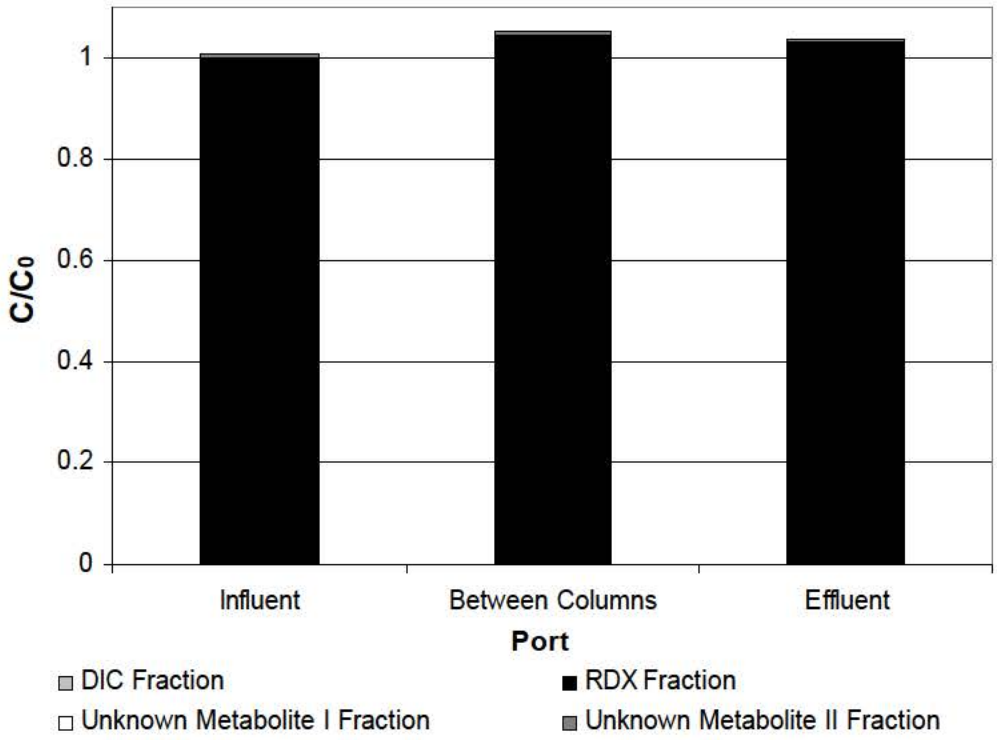

Fig. 29. ^{14}C activity after 3 months operation for control columns packed with inert glass bead media.

The ^{14}C data shows significant mineralization through the soil column, proving that natural attenuation down-gradient of a PRB contributes to PRB treatment reliability and robustness. This corroborates our general hypothesis that RDX can be effectively removed by iron PRBs and that process performance can be enhanced by the simultaneous of r subsequent participation of some microorganisms. The contact time through the iron layer was only about 40 minutes, reflecting the high reactivity of Fe(0) towards RDX and suggesting that PRBs that treat RDX plumes could be thinner than those installed to intercept chlorinated solvents. A quantitative depiction of these findings is shown below in figure 4.

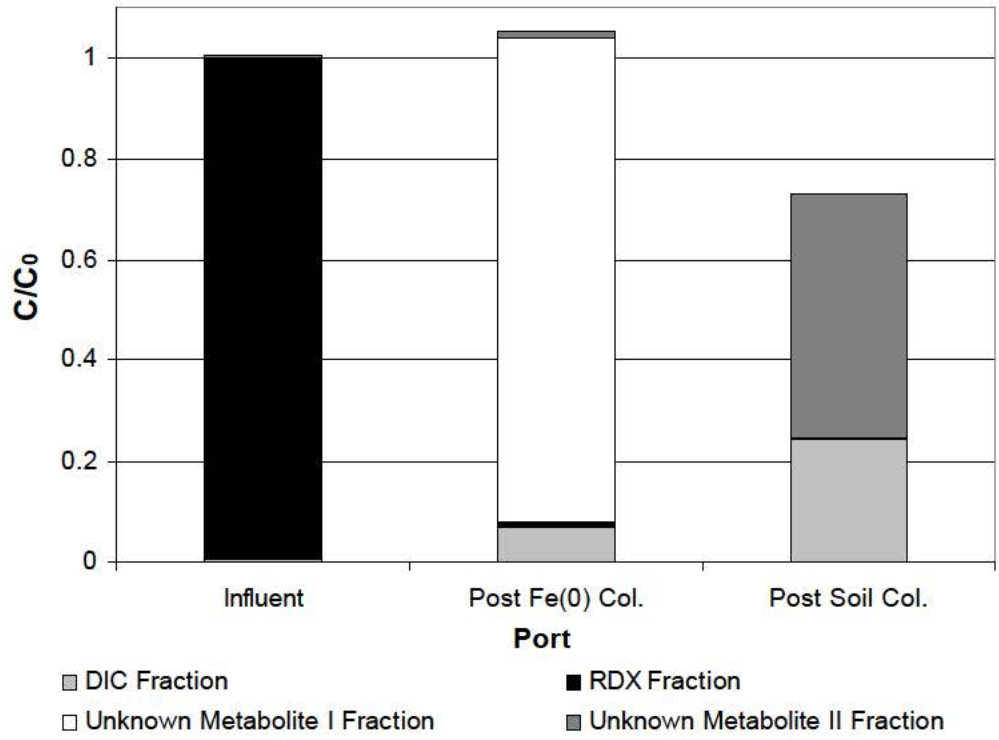

Fig. 30. ^{14}C activity after 3 months operation for experimental columns.

The figure shows how most of the ^{14}C activity is present in an unknown metabolite I after the iron barrier. This is consistent with data previously reported concerning the reactivity of RDX and permeable reactive iron barriers. Almost no RDX escape this barrier, and a small amount of it is mineralized to carbon dioxide in the iron barrier. Most exists as this unknown metabolite. This metabolite might likely be hydroxylamino-dinitroso-1,3,5-triazine (DNX) or hydroxylamino-nitroso-1,3,5-triazine (MNX) (Adrian 2001), and this will be determined in the future.

The ^{14}C activity after the soil column, however, is present mainly as carbon dioxide and a different unknown metabolite II. This shows that the bacterial population in soil downgradient of a PRB has the capability to mineralize contaminant byproducts that escape an iron barrier. It

is suggested by these data that all escaping compounds might be degraded when allowed adequate time. This would suggest that in field procedure, monitoring of PRB or RDX need only show that no RDX escapes the barrier. All byproducts should eventually be naturally attenuated in the soil downgradient of the PRB.

Furthermore, this study shows that the unknown metabolite produced by from RDX reduction by Fe(0) is not toxic to microbes in soil, at least not at the levels tested. It should follow that dilution effects caused by groundwater dispersion should eventually provide a sufficiently low concentration of this metabolite so that it may be naturally attenuated in soil.

SUMMARY OF MAJOR ACCOMPLISHMENTS

1. Flow-through Fe(0) columns inculated with municipal anaerobic sludge (simulating bioaugmented permeable reactive barriers) continue to efficiently remove RDX. This bioaugmented Fe(0) is proving sustainable for treatment of RDX as columns have now been operation for greater than two years. Analysis of ^{14}C-RDX and soluble ^{14}C metabolites shows the continued ability of these columns to degrade RDX, and likely mineralize RDX, after 32 months operation. Investigation of the hydraulic characteristics of these columns also shows little or no change in the porosity of biologically active iron columns showing the sustained performance of these simulated barriers. This provides further evidence of the sustainability of the combined iron and microbiological community to remain active as an RDX treatment system.
2. The presence of homoacetogenic bacteria in actively-degrading RDX columns containing iron has been previously demonstrated. Therefore, the ability of

homoacetogenic bacteria to directly utilize RDX was investigated. Experiments using *Acetobacterium paludosum* showed that this bacterium was capable of converting RDX, but was incapable of mineralizing RDX to CO_2 and N_2O as previously observed for anaerobic sludge. It has been further proposed that homoacetogens could conduct primary productivity, converting cathodic hydrogen and bicarbonate to form acetate. This could be an important role in biological-iron systems, since acetate could stimulate heterotrophic activity. Batch experiments show these homoacetogenic bacteria degrade but do not mineralize RDX, and may be capable of using RDX as a nitrogen source.

3. Batch experiments showed that sulfate green rust, a highly-reactive iron oxide, is capable of completely degrading RDX. The predominant end-product observed from these transformations was formaldehyde (HCHO). The recovery of formaldehyde seems to account for at least one of the previously unidentified RDX soluble metabolites formed in these RDX-degrading systems. Ammonium (NH_4^+) and nitrous oxide (N_20) were the predominant nitrogen products recovered in these experiments.

4. Mineralization assays were conducted with soluble RDX-degradation byproducts from two different RDX-treatment schemes to assess the potential for natural attenuation of RDX metabolites that could break through an iron barrier. ^{14}C-labeld byproducts were obtained from (i) the effluent of a bioaugmented iron column and (ii) batch reactors with pure cultures of *Acetobacterium paludosum.* The ^{14}C-labeld byproducts were mineralized faster and to a greater extent than the ^{14}C-RDX under both aerobic and anaerobic conditions. Higher extent of mineralization occurred

under anaerobic conditions. This is significant as it suggests the potential for complete mineralization of RDX by an integrated PRB-ZVI with downgradient natural attenuation scheme.

5. Flow-through columns with bioaugmented Fe(0) (simulating bioaugmented ZVI-PRB) continue to efficiently remove RDX. Columns containing "aged" iron (previously reacted with oxidized pollutants other than RDX (Cr(VI), TCE, and nitrate) were operated for greater than one year. Two columns were bioaugmented with DIRB *Shewanella algae* BrY or *Geobacter metallireducens* GS-15 to investigate the potential for enhancing the reactivity of aged iron by DIRB through reductive dissolution of passivating iron oxides or though production of biogenic reactive minerals. All columns showed complete degradation of RDX that was sustained over the duration of the experiment and also showed an increase in removal of soluble RDX-degradation metabolites (likely resulting from mineralization). The greatest influence of bioaugmentation with DIRB cultures to these columns appears to have been during the initial months of operation where removal of soluble ^{14}C was observed more rapidly in bioaugmented columns. Nonetheless, the ability of DIRB to affect complete mineralization (by generating reactive iron species) in zones downstream of a permeable reactive iron barrier requires further investigation.

6. Production of nitrous oxide (N_2O) was confirmed for the homoacetogen, *Acetobacterium paludosum* incubated with RDX, suggesting cleavage of the RDX ring. *A. paludosum* was also apparently able to utilize RDX as a nitrogen source, and RDX degradation was inhibited by NH_4^+, a more labile N source.

7. Batch studies were conducted to determine the ability of BrY to utilize RDX as a nitrogen source. It was found that BrY can utilize the PIPES biological buffer as a nitrogen source, which confounded interpretation of the results. The presence of this buffer in previous experiments might have inhibited the rate of RDX degradation by BrY.

8. Flow-through columns consisting of a Fe(0) column preceding a column packed with unsterilized soil were conducted to evaluate the feasibility of an integraded PRB-natual attenuation approach to intercept and treat RDX plumes. This study showed that byproducts of RDX reduction by Fe(0) that might escape a PRB can be readily mineralized by microbes naturally found in soil. This suggests that natural attenuation of RDX byproducts increases the robustness of PRBs, and that relatively thin (and less costly) barriers could be installed to transform RDX and promote its subsequent microbial mineralization.

.

PUBLICATIONS FROM THIS GRANT

Journal Articles

Oh B-T and P.J.J. Alvarez (2003). Removal of explosives using an integrated Fe^0-microbial treatment in flow-through columns. Bulletin of Environmental Contamination and Toxicology (Submitted)

Ginner J.L., P.J.J. Alvarez, S.L. Smith, and M.M. Scherer (2003). Nitrate and Nitrite reduction by Fe^0: influence of mass transport, temperature, ph, and denitrifying microbes. Environ. Eng. Sci. (In press).

Oh B-T and P.J.J. Alvarez (2002). Hexahydro-1,3,5-Trinitro-1,3,5-Triazine (RDX) degradation in biologically active iron columns. Water, Air Soil and Soil Pollution 141 (1-4): 325-335.

Oh, B-T., C.L. Just, and P.J.J. Alvarez (2001). Hexahydro-1,3,5-Trinitro-1,3,5-Triazine (RDX) mineralization by zero-valent iron and mixed anaerobic cultures. Environ. Sci. Technol. 35(21):4341-4346

Abstracts, Conference Proceedings, and Presentations

Sutton B. and P. J.J. Alvarez (2004). RDX degradation by *Shewanella algae* BrY and by its biogenic iron mineral. Proc. In Situ and On-Site Bioremediation: 4th International Conference of Chlorinated and recalcitrant Compounds, Monterey, CA, May 24-27, 2004.

Shrout J.S., P. Larese-Casanova, M. M. Scherer, and P. J.J. Alvarez (2004). Sustained RDX degradation in bioaugmented, simulated Fe(0) permeable reactive barriers. Proc. In Situ and On-Site Bioremediation: 4th International Conference of Chlorinated and recalcitrant Compounds, Monterey, CA, May 24-27, 2004.

Diels L., L. Bastiaens, S. O'Hannessin, J. L. Cortina, P. J. Alvarez, M. Ebert, and H. Schad (2003). Permeable Reactive Barriers: a multidisciplinary approach of a new emerging sustainable groundwater treatment technology. Proc. ConSoil2003. Ghent, Belgium, May 12-16, 2003.

Gregory K.B., A.B. Williams., P.J.J. Alvarez, G.F. Parkin, and *M.M. Scherer* (2003). RDX transformation in the presence of ferrihydrite and *Geobacter metallireducens* GS-15.

Proc. In Situ and On-Site Bioremediation: 7th International Symposium, Orlando, FL, June 2-5, 2003.

Gregory, K. B., B.-T. Oh, P. J. J. Alvarez, M. M. Scherer and G. F. Parkin (2001). Biogeochemical Removal of RDX Using Iron Oxide and *Geobacter metallireducens* GS-15. Proc. In Situ and On Site Bioremediation: 6th International Symposium, San Diego, CA June 4-7, 2001.

Scherer M.M., P. Larese-Casanova, K.B. Gregory, P.J. Alvarez, and G.F. Parkin (2003). Fate of RDX in the presence of reduced Fe oxides. "In Preprints Extended Abstracts (Env. Chem. Division), American Chemical Society, 225th National Meeting, New Orleans, LA

2003 MILESTONES
Project No. CU1231

		Planned Completion	Status
Task 1:	**Pathway Analysis—Identification of Unknown Metabolite(s)**		
	1.0 Partitioning Characteristics (Volatility and K_{ow})	4/2003	Completed
	2.0 LC/MS Analysis of Metabolite	12/2003	Completed
Task 2:	**Column Studies—Evaluate Column Efficiency and Sustainability**		
	1.0 Monitor RDX Removal and Mineralization	12/2003	Completed
	2.0 Determine Final RDX and Byproduct Concentration Profiles (in Aged Fe(0) Columns)	3/2003	Completed
	3.0 Determine Changes in Effective Porosity and Dispersion	12/2003	Completed
	4.0 Evaluate Efficacy of Integrated Fe(0) Barrier-Monitored Natural Attenuation to remove RDX byproducts	12/2003	Completed
Task 3:	**RDX degradation by Iron Oxides**		
	1.0 Degradation of RDX by Reduced Fe Minerals	9/2003	Completed
Task 4:	**Characterization of a Microbial Community in Fe(0) Samples**		
	1.0 Characterize Bacterial Community by DGGE	6/2003	Completed
	2.0 Characterize Iron Oxides by Mössbauer	6/2003	Completed
	3.0 Investigation of Homoacetogens	7/2003	Completed
	4.0 Investigation of *Shewanella algae* BRY	12/2003	Completed

REFERENCES

Adrian, N. R. and T. Chow (2001). Identification of hydroxylamino-dinitroso-1,3,5-triazine as a transient intermediate formed during the anaerobic biodegradation of hexahydro-1,3,5-trinitro-1,3,5-triazine. Environmental Toxicology and Chemistry **20**: 1874-1877.

Adrian, N. R. and A. Lowder (1999). Biodegradation of RDX and HMX by a methanogenic enrichment culture. Bioremediation of Nitroaromatic and Haloaromatic Compounds. B. C. Alleman and A. Leeson. Columbus, OH, Battelle Press: 1-6.

Ampleman, G., S. Thiboutot, J. Lavigne, A. Marois, J. Hawari, A. M. Jones and D. Rho (1995). Synthesis of C-14-labeled hexahydro-1,3,5-trinitro-1,3,5-triazine (RDX), 2,4,6-trinitrotoluene (TNT), nitrocellulose (NC) and glycidylazide Polymer (GAP) for use in assessing the biodegradation potential of these energetic compounds. Journal of Labeled Compounds & Radiopharmiceuticals **36**: 559-577.

Bhushan, B., A. Halasz, J. Spain, S. Thiboutot and J. Hawari (2002). Biotransformation of hexahydro-1,3,5-trinitro-1,3,5-triazine by a NAD(P)H: Nitrate oxidoreductase from *Aspergilus niger*. Environmental Science and Technology (in press).

Das, A. and F. Caccavo, Jr. (2000). Dissimilatory Fe(III) oxide reduction by *Shewanella alga* BrY requires adhesion. Current Microbiology **40**: 344-347.

Fredrickson, J. K. and Y. A. Gorby (1996). Environmental process mediated by iron-reducing bacteria. Current Opinion in Biotechnology **7**: 287-294.

Good, N. E. and S. Izawa (1968). Hydrogen ion buffers. A. San Pietro. New York, Academic. **24:** 53-68.

Gorby, Y. A., and H. Jr., Bolton (1993). Effects of O_2 on metal-reductase activity and cytochrome content in a facultative Fe(III)-reducing bacterium. Abstracts of the Annual Meeting of the American Society for Microbiology **37**.

Gregory, K. B., B.-T. Oh, M. M. Scherer, G. F. Parkin and P. J. J. Alvarez (2000). Biogeochemical degradation of redox-sensitive compounds using iron oxide and *Geobacter metallireducens* GS-15. 220th American Chemical Society National Meeting, Washingto D.C., ACS.

Gregory, K. B., M. Von Arb, P. J. J. Alvarez, M. M. Scherer and G. F. Parkin (2001). Biogeochemical removal of RDX using iron oxide and *Geobacter metallireducens* GS-15. Bioremediation of Energetics, Phenolics, and Polycyclic Aromatic Hydrocarbons. V. S. Magar, G. Johnson, S. K. Ong and A. Leeson. Colombus, OH, Battelle Press: 1-9.

Gu, B.; Phelps, T. J.; Liang, L.; Dickey, M. J.; Roh, Y.; Kinsall, B. L.; Palumbo, A. V.; Jacobs, G. K. 1999. Biogeochemical dynamics in zero-valent iron columns: Implications for permeable reactive barriers. *Environ Sci Technol* **33**:2170-2177.

Halasz, A., J. Spain, L. Paquet, C. Beaulieu and J. Hawari (2002). Insights into the formation and degradation mechanisms of methylenedinitramine during the incubation of RDX with anaerobic sludge. Enironmental Science and Technology **36**(4): 633-638.

Hawari, J., A. Halasz, T. W. Sheremata, S. Beaudet, C. Groom, L. Paquet, C. Rhofir, G. Ampleman and S. Thiboutot (2000). Characterization of metabolites during biodegradation of hexahydro-1,3,5-trinitro-1,3,5-triazine (RDX) with municipal anaerobic sludge." Applied and Environemntal Microbiology **66**(6): 2652-2657.

Hofstetter, T. B., C. G. Heijman, S. B. Haderlein, C. Holliger and R. P. Schwarzenbach (1999). Complete reduction of TNT and other (poly)nitroaromatic compounds under iron-reducing subsurface conditions. Environmental Science and Technology **33**: 1479-1487.

Kotsyurbenko, O. R. et al. (1995). New species of psychrophilic acetogens: *Acetobacterium bakii* sp. nov., *A. paludosum* sp. nov., *A. fimetarium* sp. nov. Arch. Microbiol. **163**: 29-34.

Lovley, D. R, S. Giovannoni, J. D. White, C. J. Champine, E. J. P. Phillips, Y. A. Gorby and S. Goodwin (1993). *Geobacter metallireducens*, gen. nov. sp. nov., a microorganism capable of coupling the complete oxidation of organic compounds to the reduction of iron and other metals. Archies of Microbiology **159**: 336-344.

Lovley, D. R. and E. J. P. Phillips (1986). Organic matter mineralization with reduction of ferric iron in anaerobic sediments. Applied and Environmental Microbiology **52**(4): 682-689.

Lovley, D. R. and E. J. P. Phillips (1986). Availability of Ferric Iron for microbial reduction in bottom sediments of the freshwater Tidal Potomac River. Applied and Environmental Microbiology **52**(4):751-757.

McCormick, M. L. and E. J. Bouwer (2002). Carbon tetrachloride transformation in a model iron-reducing culture: Relative kinetics of biotic and abiotic reactions. Environmental Sceience and Technology **36**(3): 403-410.

Oh, B. -T., C. L. Just and P. J. J. Alvarez (2001). Hexahydro-1,3,5-trinitro-1,3,5-triazine mineralization by zerovalent iron and mixed anaerobic cultures. Enironmental Science and Technology **35**(21): 4341-4346.

Oh, B. –T and P. J. Alvarez (2002). Hexahydro-1,3,5-trinitro-1,3,5-triazine (RDX) degradation in biologically-active iron columns. Water, Air and Soil Pollution **141**: (in press).

Rajagopal, B. S. and J. LeGall (1989). Utilization of cathodic hydrogen by hydrogen-oxidizing bacteria. Applied Microbiology and Biotechnology **31**: 406-412.

Reardon, E. J. 1995. Anaerobic Corrosion of Granular Iron - Measurement and Interpretation of Hydrogen Evolution Rates*Environ Sci Technol* **29 :** 2936-2945.

Sheremata, T. W. and J. Hawari (2000). Mineralization of RDX by the white rot fungus *Phanerochaete chrysosporium* to carbon dioxide and nitrous oxide. Environmental Science and Technology **34**: 3384-3388.

Stookey, L. L. (1970). Ferrozine-a new spectrophotometric reagent for iron. Anal. Chem. **42**: 779-781.

Taylor, R. M. (1980). Formation and properties of Fe(II)Fe(III) hydroxy-carbonate and its possible significance in soil formation. Clay Minerals **15**: 369-382.

Vikesland, P. J. and R. L. Valentine (2000). Reaction pathways involved in the reduction of monochloramine by ferrous iron. Environmental Science and Technology **34**(1): 83-90.

von Gunten U. and J. Zobrist (1993). Biogeochemical changes in groundwater-infiltration systems: columns studies. Geochim. Cosmochim. Acta **57**: 3895-3906.

Warren, L. A. and G. F. Ferris (1998). Continuum between sorption and precipitation of Fe(III) on microbial surfaces. Environmental Science and Technology **32**(15): 2331-2337.

Williams, A. G. B. and M. M. Scherer (2001). Kinetics of Cr(VI) reduction by carbonate green rust. Environmental Science & Technology **35**(17): 3488-3494.

Zhao JS, Halasz A, Paquet L, Beaulieu C, Hawari J. 2002. Biodegradation of hexahydro-1,3,5-trinitro-1,3,5-triazine and its mononitroso derivative hexahydro-1-nitroso-3,5-dinitro-1,3,5-triazine by Klebsiella pneumoniae strain SCZ-1 isolated from an anaerobic sludge. *Appl Environ Microbiol.* **68**(11):5336-41.